

NUDT4MSTAR: A New Dataset and Benchmark Towards SAR Target Recognition in the Wild

Yongxiang Liu*, Weijie Li, Li Liu*, Jie Zhou, Xuying Xiong, Bowen Peng, Yafei Song, Wei Yang, Tianpeng Liu, Zhen Liu, Xiang Li*

Abstract—Synthetic Aperture Radar (SAR) stands as an indispensable sensor for Earth observation, owing to its unique capability for all-day imaging. Nevertheless, in a data-driven era, the scarcity of large-scale datasets poses a significant bottleneck to advancing SAR automatic target recognition (ATR) technology. This paper introduces NUDT4MSTAR, a large-scale SAR dataset for vehicle target recognition in the wild, including 40 target types and a wide array of imaging conditions across 5 different scenes. NUDT4MSTAR represents a significant leap forward in dataset scale, containing over 190,000 images—tenfold the size of its predecessors. To enhance the utility of this dataset, we meticulously annotate each image with detailed target information and imaging conditions. We also provide data in both processed magnitude images and original complex formats. Then, we construct a comprehensive benchmark consisting of 7 experiments with 15 recognition methods focusing on the stable and effective ATR issues. Besides, we conduct transfer learning experiments utilizing various models trained on NUDT4MSTAR and applied to three other target datasets, thereby demonstrating its substantial potential to the broader field of ground objects ATR. Finally, we discuss this dataset's application value and ATR's significant challenges. To the best of our knowledge, this work marks the first-ever endeavor to create a large-scale dataset benchmark for fine-grained SAR recognition in the wild, featuring an extensive collection of exhaustively annotated vehicle images. We expect that the open source of NUDT4MSTAR will facilitate the development of SAR ATR and attract a wider community of researchers.

Index Terms—Synthetic aperture radar (SAR), automatic target recognition (ATR), classification, detection, dataset, benchmark

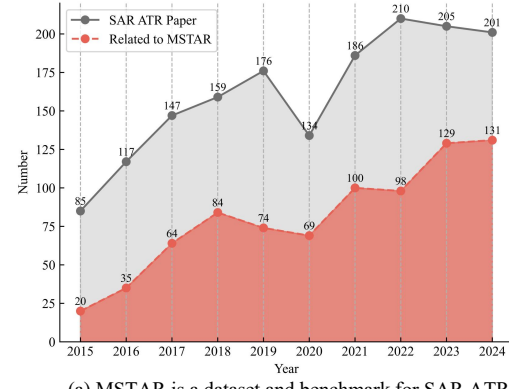
INTRODUCTION

CAN humans perceive and recognize objects on the Earth beyond the limitations of optical vision using microwave vision [20]? Synthetic aperture radar (SAR) [61, 72], an active imaging sensor, acquires the ground scattering characteristics by emitting the electromagnetic microwave. It has emerged as an indispensable tool for information acquisition in Earth observation and target surveillance [20, 22, 76], as its resolution remains unaffected by the observation distance or lighting conditions. Moreover, it has the advantage of operating effectively in various weather conditions. SAR interpretation has witnessed remarkable progress, propelled by the advancement of high-resolution imaging and artificial intelligence technologies [20, 64]. SAR automatic target recognition (ATR), which autonomously detects and classifies objects of interest (e.g., vehicles, ships, aircraft, and buildings) within imagery, is a critical frontier in advancing the capabilities of SAR interpretation. It has various civil and military applications such as urban management, disaster assessment, emergency rescue, and global surveillance [18, 25, 44, 49, 98]. Since the 1970s, researchers have been dedicated to developing a generalized stable SAR ATR system. However, the recognition of objects from SAR imagery have encountered significant challenges.

Special characteristics. SAR imagery has special electromagnetic scattering attributions but is devoid of common features such as color and texture typically present in human vision. The scattering properties of targets are highly influenced by a multitude of factors, including the imaging angle, resolution,

*This work was supported by the National Natural Science Foundation of China under Grant 62376283, the Science and Technology Innovation Program of Hunan Province under Grant 2022RC1092, and the Key Stone Grant JS2023-03 of the National University of Defense Technology. (*Corresponding authors: Xiang Li, Yongxiang Liu, and Li Liu. E-mail address: lixiang01@vip.sina.com, lyx_bible@sina.com, and liuli_nudt@nudt.edu.cn)*

The authors are with the College of Electronic Science and Technology, National University of Defense Technology, Changsha, 410073, China.



(a) MSTAR is a dataset and benchmark for SAR ATR

	MSTAR	NUDT-MSTAR
Year	1995	2025
# Classes	8	21
# Types	10	40
Location	ideal centered	random non-centered
Scene	grass	5 simple & difficult scenes
Band	X	X, Ku
Polarization	single	quad
Annotaion	classification	classification, detection
# Img.	14,557	194,324

(b) NUDT-MSTAR will be a new dataset and benchmark for SAR ATR

Fig. 1: Motivation of our NUDT4MSTAR. Subfigure (a) shows the number of articles on SAR ATR in the last decade. As the first SAR target classification dataset, MSTAR has been the mainstream data benchmark. Subfigure (b) illustrates the data diversity of NUDT4MSTAR compared to MSTAR and its potential to become a new data benchmark.

polarization, background, and the geometry structure and material of targets themselves [39, 67]. Additionally, SAR images suffer quality issues, such as speckle noise, geometric distortion, and image Defocus. These factors make it difficult to interpret

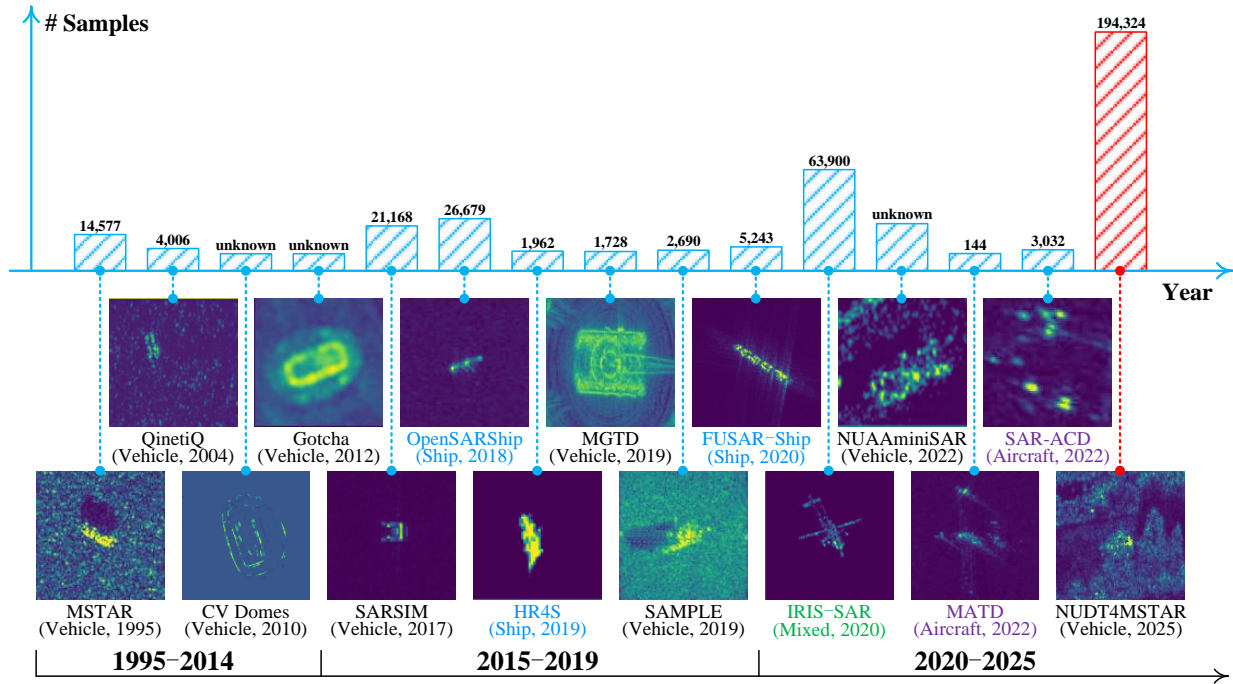


Fig. 2: Timeline of SAR classification dataset. Compared to other datasets focusing on target slices in simple scenes, we provide diverse target samples from different scenes to study the more difficult issues, and it is a much larger SAR ATR dataset.

SAR data, a recognition system independent of human vision.

Insufficient samples. Acquiring SAR images encompassing many categories under diverse operating conditions presents a significant challenge, and annotating SAR images is considerably more costly and labor-intensive than RGB images. Three decades have elapsed since the advent of the first SAR classification dataset in the 1990s, the Moving and Stationary Target Acquisition and Recognition (MSTAR) [2] in Fig. 2. The largest publicly accessible SAR target classification dataset remains limited to a small set of no more than 30,000 images. Besides, recent target classification datasets (OpenSARShip [30] and FUSAR-Ship [29]) have severe sample imbalance, ranging from a few to thousands of samples per class. A substantial amount of work remains to be undertaken for SAR target datasets.

Nonstandard benchmarks. A standardized dataset and experimental settings serve as the north star for developing advanced SAR ATR techniques. However, the mainstream MSTAR dataset in Fig. 1 has dozens of distinct experimental settings, and existing algorithms have nearly reached near-saturation performance on this ideal benchmark [39]. Other classification datasets, such as OpenSARShip and FUSAR-Ship, also exhibit different experimental settings and dataset splitting. Moreover, the limiting access to non-open-source dataset settings and methods further intensifies this challenge.

Researchers have struggled to construct a large number of SAR target datasets to study generalized stable SAR ATR algorithms. Over the past few years, there has been a remarkable surge in remote sensing datasets across various modalities, including visible light [4, 51], SAR [52, 85], infrared [90], and multimodal [58]. As depicted in Fig. 2, recent SAR classification

datasets have significantly improved data diversity. In particular, SAR detection datasets [52, 85] with 100,000 images have emerged. Yet, regarding SAR target recognition, no dataset has emerged that can completely surpass the MSTAR benchmark dataset, released in the 1990s, regarding the diversity of target types, imaging conditions, and data formats it offers. Notably, the lack of open-source availability, inadequate samples, long-tailed distributions, unabundant collection conditions, and independent experimental settings are still all issues that warrant attention. We suggest that a large-scale fine-grained SAR target dataset and benchmarks to investigate the electromagnetic scattering properties of targets across diverse conditions represent a critical and enduring endeavor.

As a first step towards building a large-scale SAR target dataset, we introduce **NUDT4MSTAR**, a fine-grained dataset for SAR vehicle target recognition in Fig. 3. In particular, NUDT4MSTAR collects 194,324 object images in the wild from 40 target types, 5 scenes, and various imaging conditions with detailed annotation². It is the largest public SAR vehicle recognition dataset, even 10 times the size of any similar vehicle dataset previously available in Fig. 2. Then, to facilitate innovation and comparisons, we build a well-designed benchmark with 7 experimental settings and 15 recognition methods. Besides, the transfer learning results of various models trained on this dataset to other datasets show that our fine-grained recognition task benefits the feature learning of different ground targets. Finally, We provide detailed analyses and discussions to explore important issues for future research.

Our work shows the huge challenges and potential in SAR recognition and provides the benchmark for stable fine-grained ATR algorithms. The dataset and benchmark are available on our GitHub at <https://github.com/waterdisappear/>

1. For counting SAR ATR papers, we use the search formula “SAR target recognition (Title) or SAR ATR (Title) or SAR target classification (Title) or SAR classification (Title) and radar (Topic) ” on Web of Science. We added “and MSTAR (Topic)” to the previous search formula to count the number related to MSTAR.

2. This dataset focuses on the fine-grained single target recognition problem in SAR ATR, *i.e.*, the image classification task, but we provide a horizontal bounding box label for the detection task.

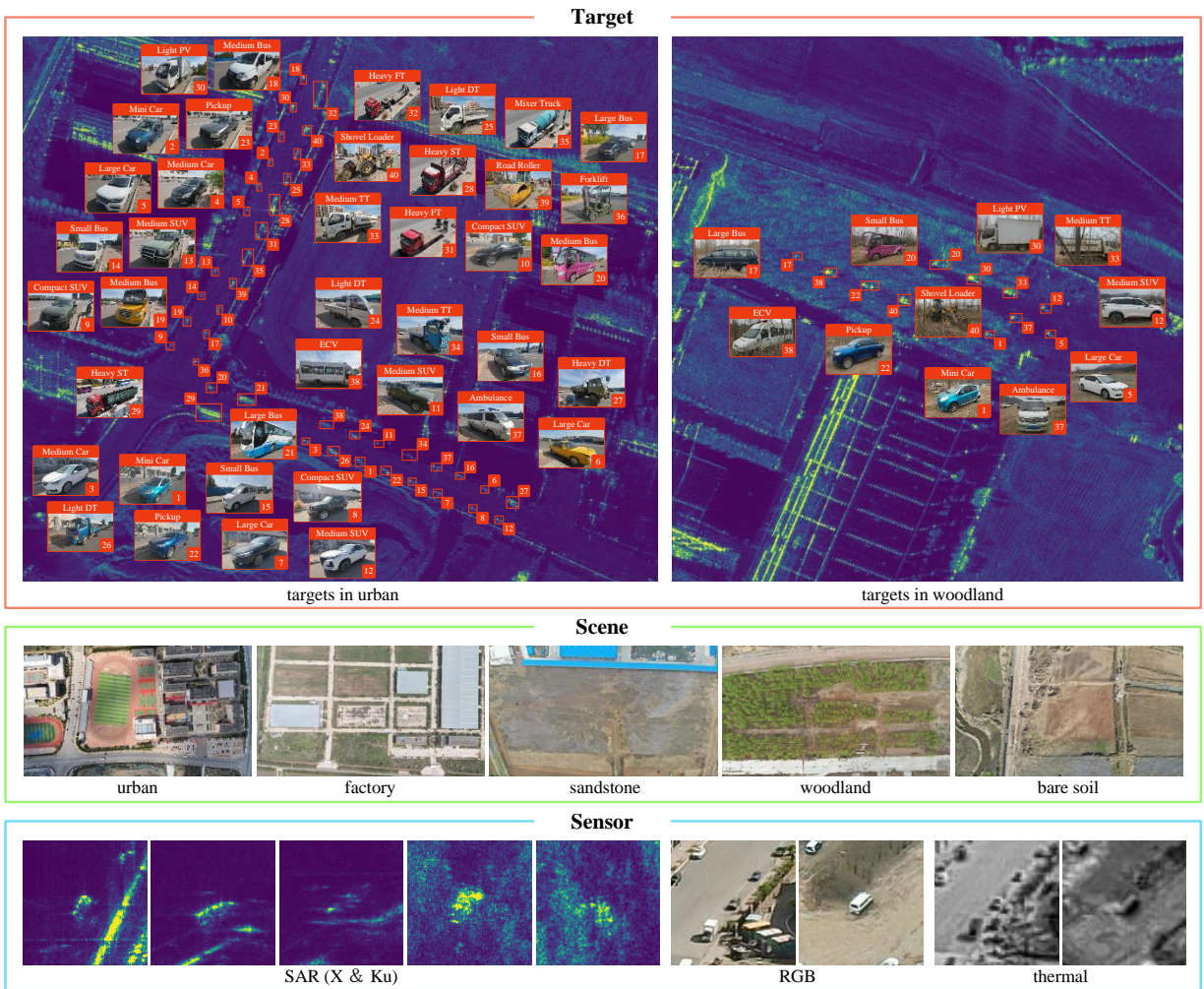


Fig. 3: **NUDT4MSTAR**. We collect target samples from 21 classes and 40 types of targets in 5 scenes with 3 modalities of sensors. Detailed target information is illustrated in Fig. 7. Due to the limitation of the scene size, there are two settings for target deployment, the first with 40 types in city, factory, and sandstone; the second with 11 types in woodland and bare soil. These vehicle types cover most current civilian vehicles in structure, size, and usage. In difficult scenarios (city and factory), vehicle positions are adjusted during acquisition to avoid pseudo-correlation between the target and the background. Although we focus on target characteristics in the SAR sensor, we also collect data from other sensors for future analysis of their differences.

NUDT4MSTAR. We believe that our new dataset, with comprehensive imaging conditions and experiment benchmark, will further promote the promise and reproducible research in SAR ATR. The main contributions of this paper are three points:

1. We build the largest dataset for SAR vehicle target recognition in microwave vision. With various target types and imaging conditions, NUDT4MSTAR not only provides a systematic study of the effects of different conditions on SAR target characteristics but also promotes the development of new ATR technologies and research topics.

2. We constructed a target classification system for this vehicle dataset, including 4 categories, 21 classes, and 40 types. A transfer learning experiment based on pre-training on this dataset shows that a large fine-grained task can provide good weight initializations for recognizing ground targets.

3. We build a comprehensive benchmark with 7 experimental settings and 15 recognition methods. This benchmark provides detailed analysis and discussion that can guide SAR recognition algorithms' designs and facilitate reproducible comparisons.

The remainder of this paper is organized as follows. Sec. 2 discusses related work in SAR target classification datasets and algorithms. Sec. 3 introduces our dataset NUDT4MSTAR. Secs. 4

conduct extensive experiments to build the benchmark. Sec. 5 concludes the paper and discusses future work.

2 RELATED WORK

Here, we review the datasets and algorithms for SAR target classification and finally discuss the significance of the datasets for algorithmic studies.

2.1 Datasets for SAR target classification

Datasets are the cornerstone of developing new techniques for SAR ATR, especially in a deep learning-based era. In the past decades, the MSTAR [2] dataset has played a key role in SAR target classification tasks. However, current deep learning-based methods are saturated on this dataset benchmark setting. MSTAR's insufficient data volume also suffers from data biases such as background correlation [39, 47]. Therefore, many datasets have been built to advance the development of this field, especially in recent years. In order to provide a comprehensive analysis, we discuss SAR target classification datasets that focus on individual target characteristics from the 1990s to the 2020s, which are detailed listed in Table 1.

TABLE 1: **Statistics of the SAR target classification datasets from the 1990s to 2020s.** We focus on the electromagnetic scattering properties of individual objects, *i.e.*, the most relevant to the classification dataset and task. Existing SAR target classification datasets face challenges such as no open source, insufficient samples, long-tailed distributions, and single collection conditions. OA.: Open access. # Classes.: Number of object classes. # Types.: Number of object types. Img. Size: image size. # Img.: Number of images. Res.: Resolution. Pol.: Polarization. “-” refers to unknown.

Dataset	Year	OA	Source	Band	Pol.	# Classes	# Types	Res. (m)	Img. Size	# Img.	Description
MSTAR [2]	1995	✓	airborne	X	single	8	10	0.3	128~193	14,557	Most cited vehicle dataset
QinetiQ [68]	2004	-	airborne	X	quad	-	9	0.3	100~150	4,006	Non-ideal background conditions
CV Domes [16]	2010	✓	simulation	X	quad	3	10	0.3	-	-	3D simulation civil vehicle
Gotcha [15]	2012	✓	airborne	X	-	7	13	0.3	-	-	3D civil vehicle dataset
SARSIM [59]	2017	✓	simulation	X	-	7	14	0.1	139	21,168	Simulation CAD vehicle
OpenSARShip [30]	2018	✓	satellite	C	dual	16	-	2.7~22	9~445	26,679	Sentinel-1 ship dataset
HR4S [3]	2019	-	satellite	C	quad	21	-	3~25	-	1,962	GF-3 and RADARSAT-2 ship
MGTD [5]	2019	-	laboratory	X	single	1	2	0.01	128	1,728	Scaled vehicle models
SAMPLE [42]	2019	✓	simulation	X	single	7	10	0.3	128	2,690	Simulation and measured pairs
FUSAR-Ship [29]	2020	✓	satellite	C	dual	98	-	1.1~1.7	512	5,243	High-resolution GF-3 ship
IRIS-SAR [1]	2020	-	simulation	-	-	8	355	-	512	63,900	Simulation CAD models
NUAAminiSAR [101]	2022	-	airborne	X	-	9	9	0.1	-	-	Multi-angle circular SAR vehicle
MATD [81]	2022	✓	airborne	Ku	-	2	2	-	128	144	Multi-angle strimap SAR aircraft
SAR-ACD [73]	2022	✓	satellite	C	single	2	6	1	32~200	3,032	GF-3 aircraft dataset
NUDT4MSTAR	2024	✓	airborne	X, Ku	quad	21	40	0.12 ~ 0.15	128	194,324	A large-scale fine-grained dataset

Vehicle dataset. Vehicle datasets usually include various types of fine-grained vehicles and imaging conditions to study the robustness classification under different distributions in the training and test sets. We summarize the target classes and types of these SAR vehicle datasets in Fig. 5. MSTAR was released by the Defense Advanced Research Projects Agency (DARPA) as the first public dataset for SAR target classification. It contains SAR image slices of 10 military vehicles and a reference target under different imaging angles with spotlight SAR. However, MSTAR has a background correlation problem and ideal collection conditions. Compared to MSTAR, the QinetiQ [68] dataset provided a non-idealized acquisition condition with a non-centered target location and stronger background clutter. CV Domes [16] and Gotcha [15] constructed simulation and measurement samples of civilian vehicles. These two datasets are in the raw echo data format and can be used for SAR imaging research, but they are not as convenient for researchers to use as MSTAR. However, these two civilian vehicle datasets are not rich in target categories and acquisition conditions. SARSIM [59] and SAMPLE [42] are two simulation datasets used to study transfer learning. In particular, SARSIM uses 14 CAD models, and SAMPLE has simulated and measured sample pairs based on partially MSTAR’s public vehicle. The simulation data have discrepancies with the measured data in background clutter, target scattering characteristics, and speckle noise. Although MSTAR includes 3 grass locations, most public images are from the same location. MGTD [5] collects the training and test sets in two different laboratory backgrounds. Another issue is that the depression angles of MSTAR public images are mostly in 15° and 17°, and some categories of images are missing at other depression angles, such as 30° and 45°. Hence, NUAAminiSAR [101] collects images of military targets at different depression angles by circular SAR in a national defense park, including 8 military vehicles and an airplane. As shown above, no vehicle datasets are sufficiently rich in target types, scene settings, and sensor conditions.

Ship dataset. SAR ship datasets have emerged with the development of satellite SAR technology. The difference with the vehicle dataset is that the ship classification dataset usually uses a satellite platform, and the imaging angles are limited. Ship datasets can be constructed and labeled with global ship tracking systems, but label noise is a difficult problem.

OpenSARShip [30], HR4S [3], and FUSAR-Ship [29] advance the development of ship classification methods. These datasets are derived from different satellites and face difficult harbor backgrounds and class imbalance challenges. OpenSARShip collects medium-resolution images of 16 classes in harbors with Sentinel-1. HR4S constructs high-resolution ship images in ports and coastal areas with GF-3 and RADARSAT-2. FUSAR-Ship contains high-resolution images under various sea backgrounds with 15 ship main classes and 98 subclasses based on GF-3. However, OpenSARShip and FUSAR-Ship have a serious class imbalance and long-tailed distribution challenges. Researchers construct various experimental settings and use some target categories for the classification based on these two datasets.

Aircraft dataset. Aircraft datasets have emerged in recent years, presenting unique challenges in remote sensing. Due to their streamlined surfaces and less obvious scattering characteristics, aircraft are more difficult to classify than vehicle and ship targets. Multiangle Aircraft Target Dataset (MATD) [81] collects SAR images of two aircraft at different imaging angles with a drone strimap SAR equipment. SAR-ACD [73] contains 2 categories and 6 types of civil aircraft in 3 airports.

Others. IRIS-SAR [1] is rich in aircraft, ships, and vehicle simulation types. It considers noise, clutter, and shadows in SAR image simulation. However, it does not take into account occlusion in complicated backgrounds.

Object detection dataset. SAR has many object detection datasets besides the classification datasets used for individual targets. These datasets are used for detecting multiple targets and have large image sizes. They contain more background interference and intensive targeting challenges. SAR object detection datasets similar to SARDet-100K [52] and FAIR-CSAR [85] with a volume of about 100,000 images are mainly satellite-based datasets, with a resolution of mostly greater than 1 m. This resolution makes it hard to detect and classify vehicle targets. Their non-cooperation objectives make it difficult to label the target types and accurately control the characteristics of the target under different angles and scenes. Therefore, our dataset provides a more fine-grained SAR vehicle characterization dataset under target class and imaging conditions.

Due to the high collection and annotation cost, collecting and publishing target samples under different imaging conditions is very difficult and time-consuming. Even after close to

thirty years since its inception, MSTAR remains the most used classification dataset. The evolution of SAR ATR necessitates a new large-scale dataset and benchmark in the new era. After the above investigation, we suggest that a good SAR ATR dataset should pay attention to the following key points.

- *Richness.* The dataset should include rich target categories, scenes, and imaging conditions to approximate the real world and reduce data bias.
- *Metadata.* The dataset needs enough metadata, such as complex data, scene description, and imaging parameters. Researchers can propose new algorithms by combining metadata with SAR image characteristics.
- *Standardization.* An official benchmark and setting are beneficial to fair comparisons across different methods. In addition, the dataset format should be compatible with mainstream datasets for expansion and scaling.
- *Usability.* The dataset should be readily accessible and user-friendly for researchers to download and utilize. Some datasets may be difficult to access or require additional SAR imaging and pre-processing steps.

Therefore, we build and open-source a new large-scale dataset, NUDT4MSTAR, with various categories and imaging conditions. This dataset is carefully labeled with extensive metadata and has an official benchmark based on 7 experimental settings and 15 comparison methods with 2 data formats. This dataset is our first step in building a new SAR target dataset system. In the future, we will expand the objects from vehicles to a wider category list to develop SAR ATR.

2.2 Review of SAR Target Classification Algorithms

Early target classification relies on hand-crafting features and classifiers, while contemporary methodologies are predominantly anchored in deep learning-based methods. According to their different feature representations, we divided target recognition methods into four distinct paradigms: traditional features, deep learning, feature fusion, and classification with metadata. In an era increasingly dominated by data-driven algorithms, the availability of a rich, standardized, and usable dataset enriched with metadata is becoming increasingly pivotal.

Traditional features. Previous studies have proposed a plethora of valuable features, encompassing geometric structure features [23, 33], electromagnetic-scattering features [11, 37, 45, 63, 93], time-frequency features [71], local descriptors [13, 70], and sparse representations [28]. These features are particularly tailored to the special coherent imaging mechanisms. For instance, SAR-HOG [70] employs a ratio-based gradient computation rather than the traditional differential gradient approach, and Attributed Scattering Centers (ASC) provides a feature set including location, geometry, and polarization information. Notably, extracting electromagnetic-scattering features relies on complex images with phase information, underscoring the necessity of providing comprehensive data formats.

Deep learning. Deep learning algorithms excel at uncovering intricate patterns within datasets, particularly when ample data is available. Nowadays, these algorithms achieve a remarkable nearly 99% accuracy on MSTAR’s basic Standard Operating Condition (SOC) settings, but the Extended Operating Condition (EOC) with robustness and few-shot are more challenging problems. Convolutional Neural Network (CNN) [40, 57] is a common network in SAR target classification. All-convolutional network (A-ConvNet) [8] was proposed to reduce overfitting

and had high accuracy under many experiment settings but is not robust to noise. In recent years, Transformer [14, 78] has also been used in SAR target classification. After a decade of significant progress, SAR target recognition now incorporates many advanced deep learning techniques such as data augmentation [12, 24, 41], attention mechanism [65, 80], domain alignment [50], reinforcement Learning [7, 35], transfer learning [89], meta-learning [21], physical deep learning [9, 32, 53, 82], semi-supervised learning [97], and self-supervised learning [34, 48, 92]. The majority of research endeavors are based on the MSTAR dataset, and a subset of studies also create the different non-open source settings of OpenSARShip and FUSAR-Ship datasets. Nonetheless, the reliance on outdated datasets and the lack of standardized benchmarks are impeding the advancement of SAR target recognition in the 2020s.

Feature fusion. In order to improve the robustness and interpretability of deep learning methods, many feature fusion methods combining traditional and deep features have been proposed. Kechagias *et al.* [38] discussed the fusion of deep Learning and sparse coding. FEC [94] used deep CNN and ASC features based on complex data with amplitude and phase. Li *et al.* [43] combined scattering centers (SC) with graph convolutional network. Besides feature fusion methods, ESF [19] applied ASC features to guide deep model training. EFTL [54] proposed using the ASC model as weight initialization of a complex convolutional network. PIHA [31] proposed a hybrid attention mechanism with ASCs and the deep learning framework. LDSF [88] constructed a heterogeneous graph for the first time to fully exploit both the scattering information of the target components and their interactions. However, many SAR target datasets only provide magnitude images, ignoring phase information and quantization issues.

Classification with metadata. Imaging angles and target-related metadata are the two most prevalent categories of ancillary data. MSTAR and SAMPLE datasets furnish the imaging angles for each respective image. RotANet [84] combined predicting the rotational pattern of an image sequence with self-supervised learning. Zhang *et al.* [95] investigated the problem of optimal image imaging angle selection in few-shot recognition based on the MSTAR dataset. AaDRL [35] explored the SAR active recognition framework to fully exploit target characteristic variations at different azimuth angles based on the SAMPLE dataset. In addition, many multi-view methods [62, 74] were proposed with image sequences from different imaging angles. Since the target types are known, the researchers used 3D models and shape parameters as metadata for fine-grained tasks. For example, SARbake [60] used 3D CAD models and projection relations for semantic segmentation, and DBAE [83] utilized size and structure attributes for zero-shot classification. Consequently, a SAR target dataset enriched with pertinent metadata, encompassing both imaging parameters and detailed target characteristics, becomes an indispensable step in pursuing accurate and robust SAR target recognition.

Experimental settings. Indeed, the MSTAR dataset has more than 50 types of experimental configurations for SOC and EOC, as detailed in [39]. These configurations include image angle variation, target version/configure variation, noise corruption, occlusion, resolution variation, and background clutter variation [39, 50]. In a similar vein, other SAR classification datasets, such as OpenSARShip and FUSAR-Ship, lack a standard experimental benchmark, and researchers also devise different bespoke settings that leverage subsets of the

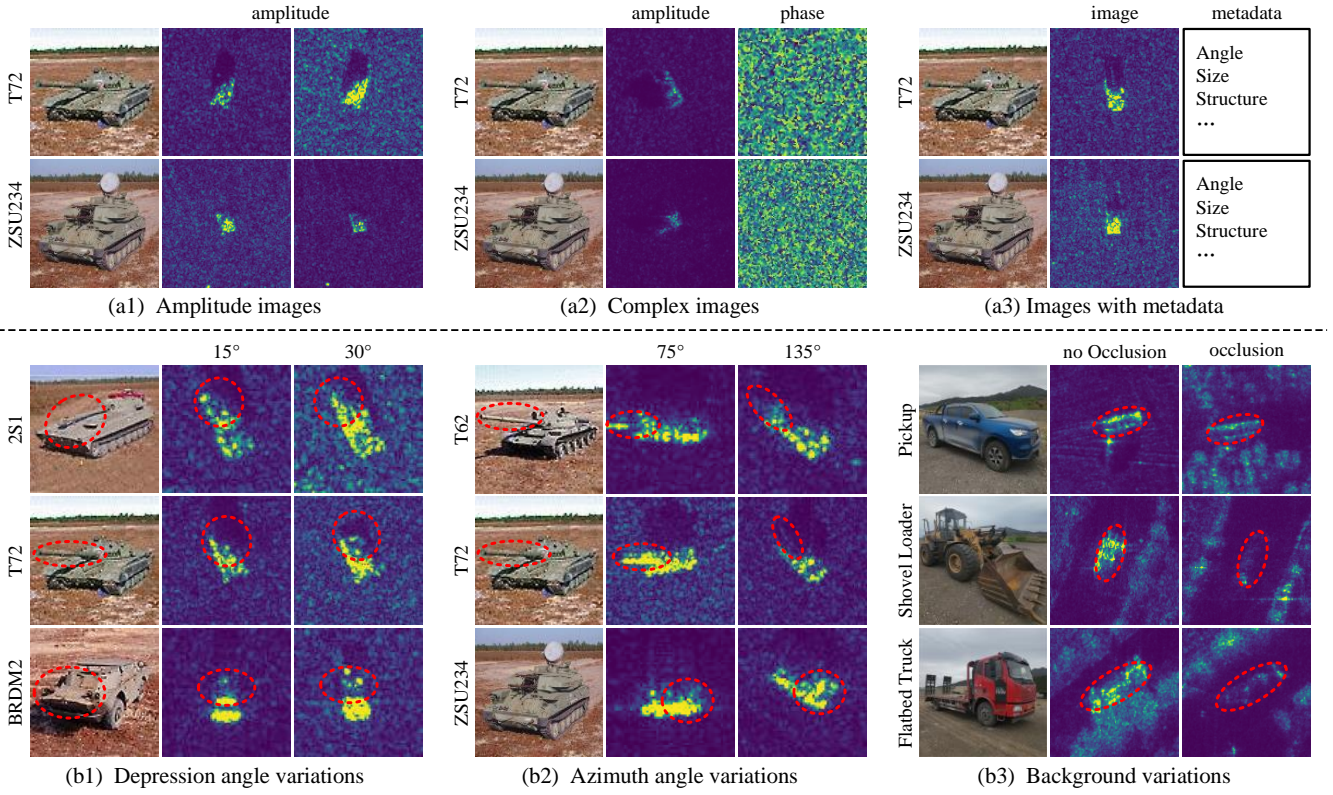


Fig. 4: Importance of Dataset. Taking the MSTAR dataset as an example, subfigures (a1)-(a3) describe the common data inputs of existing algorithms. The MSTAR dataset provides processed magnitude data, raw complex data, and corresponding metadata. Therefore, this dataset remains the most used one over two decades after its release. Subfigures (b1)-(b2) show its mainstream experimental settings that are based on various imaging conditions of the MSTAR dataset. Other experimental settings include target configuration/version variation and simulation settings (simulation noise erosion and occlusion) [50]. However, the limited number of MSTAR categories and acquisition conditions restrict the further study of the SAR ATR. For example, the current occlusion usually uses zero values to fill some image regions, but the real occlusion in our measured dataset subfigure (b3) is not the same as the existing simulation. Therefore, building a new large-scale fine-grained vehicle dataset in the 2020s is necessary for the development of SAR target recognition based on the strengths of the previous datasets. (pseudo-color for better visualization of SAR magnitude images, and subfigures (b) are cropped for better visualization of target signature variations.)

target class for classification [32, 53].

Evaluation metrics. Classification accuracy and confusion matrix are the primary metrics employed for evaluating the performance of classification models. Accuracy quantifies the proportion of correctly classified samples relative to the total number of samples in the dataset. The confusion matrix describes the correspondence between the classification result and the ground truth. Within this matrix, each column corresponds to the predicted class labels, whereas each row represents the true class labels. Besides, the Receiver Operating Characteristic (ROC) curve is a valuable tool for assessing used for binary classification and detection tasks such as suppressing background clutter and outlier rejection [8].

We noticed a pronounced preference for the MSTAR dataset among SAR classification algorithms. Most algorithms are based on the MSTAR dataset, with a small number using other datasets such as SAMPLE, OpenSARShip, and FUSAR-Ship. This preference is attributed to the distinctive benefits of the MSTAR dataset released in the 1990s. As depicted in Fig. 4 (a), studies requiring complex data have opted for the MSTAR dataset, whereas other datasets that only provide magnitude data cannot be used to validate their algorithms. In addition, information about vehicle types in the dataset is also available on the web. Compared to other datasets with long-tailed distributions, the MSTAR dataset has a more balanced target sample and diverse imaging conditions, which facilitates the establishment of experimental frameworks and the investigation of recognition challenges. Therefore, MSTAR has accumulated a large number

of algorithms and experimental settings. However, this dataset has not released all target samples, and the extant algorithms have achieved peak performance in prevalent settings, such as classification with ten target types, imaging angle variation, and version variation. The ideal acquisition conditions of the MSTAR dataset cannot show that the recognition problem is truly well solved. Scholars are endeavoring to address these limitations by proposing novel experimental settings and datasets. However, as shown in Fig. 4 (b), some simulation experimental settings based on measured data may not accurately reflect the real world. Besides, the sample diversity is difficult to ensure due to collection and labeling costs. Therefore, we perceive a constraint on advancing SAR ATR techniques due to data limitations. Constructing a new open-source dataset benchmark with diverse target categories and imaging conditions is the cornerstone of excellent and stable SAR ATR techniques.

3 NUDT4MSTAR

The emergence of new datasets and papers has led to rapid progress in various areas of SAR ATR, demonstrating the attention given to this issue in recent years. However, a large-scale dataset with various target categories and imaging conditions is still lacking because of SAR's expensive costs and annotation. We aim to achieve as much diversity as possible in target categories, scene settings, and sensor conditions. With this in mind, our dataset has huge potential to advance the field of SAR ATR significantly. Its values for SAR ATR are:

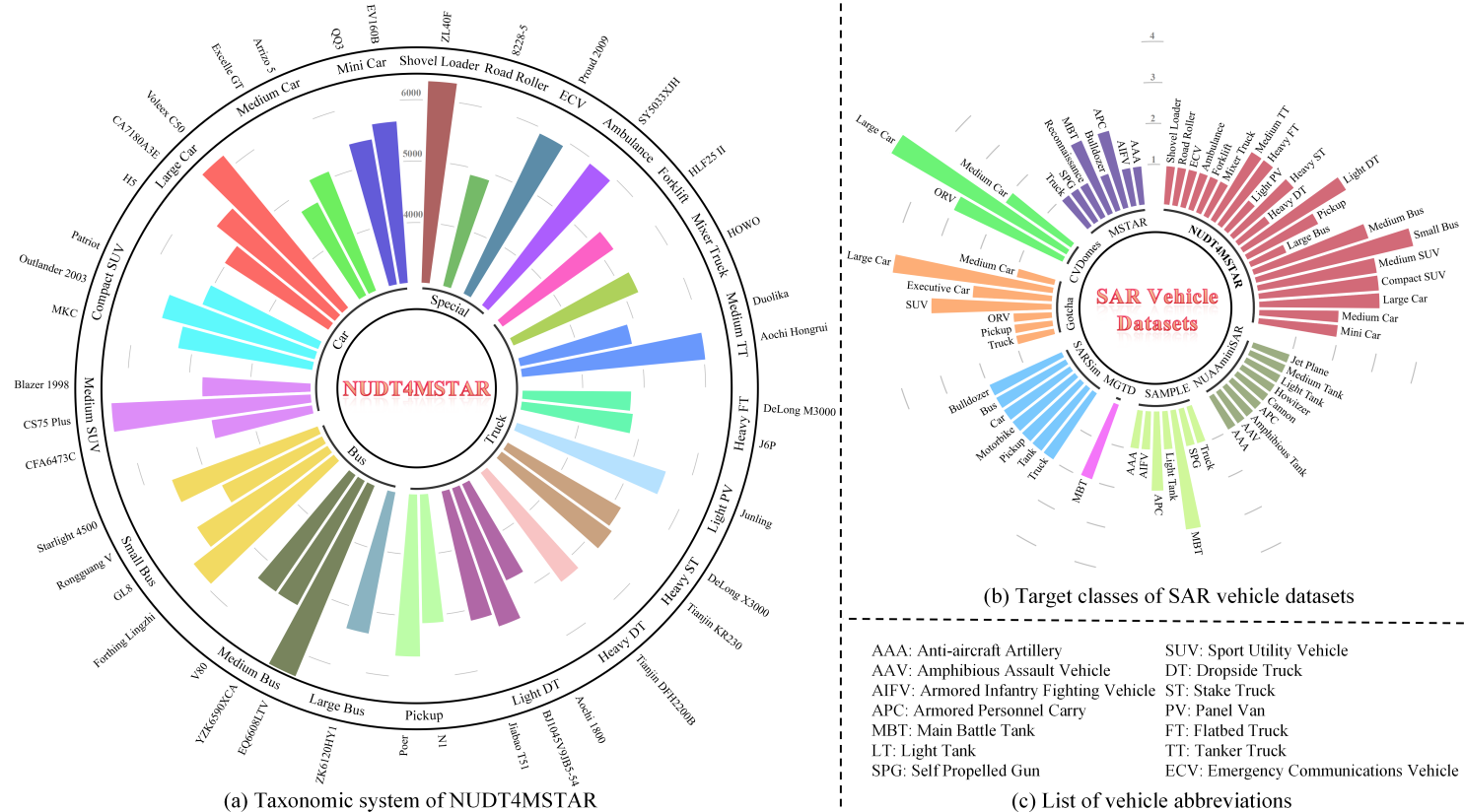


Fig. 5: **Taxonomic systems of NUDT4MSTAR.** For civilian vehicles, the taxonomy is based on Chinese and European vehicle classification standards [17, 75], according to the vehicle's purpose, structure, size, and mass. For military vehicles, we followed the MSTAR taxonomic system [67]. **(a) Taxonomic systems of NUDT4MSTAR.** Our dataset is a comprehensive civilian vehicle map covering 4 main categories, 21 classes, and 40 types. We provide a detailed illustration of the histogram distribution for these 40 vehicle types, demonstrating the breadth and depth of our dataset. Its sufficient and balanced samples make it well-equipped to meet various experimental settings and studies. **(b) Target classes of SAR vehicle datasets.** We statistically analyze the number of civilian and military vehicle classes and types in SAR vehicle datasets. Our dataset greatly enhances the civilian vehicle richness for the SAR ATR, compared to the measured dataset Gotcha and the simulated datasets CVDom and SARSim. **(c) List of vehicle abbreviations.**

TABLE 2: **Statistics of NUDT4MSTAR.** We segment the targets with fixed-size slices and random offsets to investigate their characteristics and aim for robust recognition under different collection conditions. We varied the target location in urban and factory scenes and collected data at the factory several times. In addition, some targets can not be labeled due to heavy occlusion. # Types.: Number of object types. Res.: Resolution. Pol.: Polarization. Dep.: Depression angle. Azi.: Target azimuth angle interval. Img. Size: image size. # Img.: Number of images in ground and slant range coordinate systems.

Scene	# Types	Platform	Mode	Band	Res. (m)	Pol.	Dep. (°)	Azi. (°)	Img. Size	# Img.
City	40	airborne	strimap	X	0.12 ~ 0.15	quad	15, 30, 45, 60	5	128	83,465
Factory	40	airborne	strimap	X & Ku	0.12 ~ 0.15	quad	15, 30, 45, 60	30	128	63,597
Sandstone	40	airborne	strimap	X & Ku	0.12 ~ 0.15	quad	15, 30, 45, 60	30	128	30,720
Woodland	11	airborne	strimap	X & Ku	0.12 ~ 0.15	quad	15, 30, 45, 60	30	128	8,094
Bare soil	11	airborne	strimap	X & Ku	0.12 ~ 0.15	quad	15, 30, 45, 60	30	128	8,448

- To provide a challenging and rich dataset for SAR vehicle recognition;
- To systematically study the effects of different conditions on SAR target characteristics;
- To give a benchmark to facilitate method innovation and comprehensive comparisons;
- To promote the development of new ATR technologies and research topics.

In this section, we describe the dataset construct program and then provide the details on NUDT4MSTAR in terms of key aspects, including data acquisition, professional system, statistical analysis, and dataset value.

3.1 Construct program

We aim to extend the dataset diversity as much as possible regarding targets, scenes, and sensors. These aspects are derived from the MSTAR's discussion [67] on SAR target characteristics.

Target. According to the Chinese and European vehicle classification standards [17, 75], First, we confirm the main target categories based on uses and structures of vehicles, including people carriers (car and bus), goods carriers (truck), and special purpose vehicles (special). Then, we subdivide each category into various target classes based on size and special structure and collect as different types as possible. Finally, NUDT4MSTAR has 4 categories, 21 classes, and 40 types. It covers the most of civilian vehicle categories and has the most richness on civil target classes compared to other SAR vehicle datasets in Fig. 5.

Scene. Most previous target datasets were collected in open scenes such as grasslands, focusing on target characteristics and lacking significant background interference. Therefore, we discuss both difficult and simple scenes³ in Fig. 10. The urban and factory have varying occlusion degrees and other strong

3. Since we mainly consider single target characteristics, discussing densely distributed targets such as car parks are not included in this version.

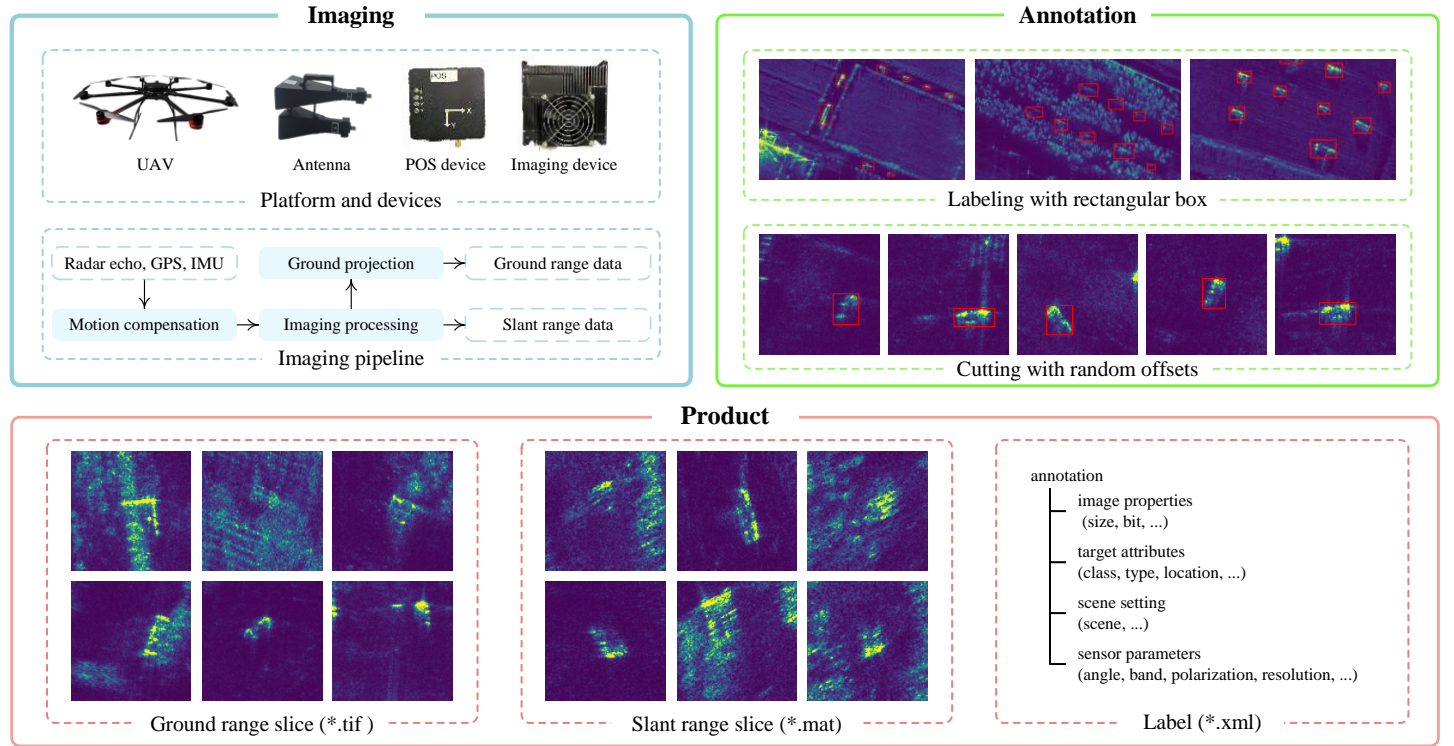


Fig. 6: **Illustrations of data acquisition.** We annotate and cut to build target slices with corresponding metadata information. The range dimension of slant range complex data is in the line of sight direction, which results in the deformation of the target shape in this dimension. Therefore, we also provide ground range images after ground projecting based on slant range amplitude data.

scattering targets, such as buildings and roadside trees. Dense trees in woodlands can weaken target scattering or increase the intensity of non-target scattering. Bare soil and sandstone are clean backgrounds, although sandstone occasionally has strong scattering background points. These interferences have a stronger effect on the target features and are more compatible with real-world challenging recognition tasks.

Sensor. The common sensor conditions are variations in depression and azimuth angle, and we collect target samples at different angles as shown in Fig. 11. We provide a balanced sample under different depression angles, including all target types, compared to MSTAR’s several targets. However, our azimuth angles are not as dense as MSTAR in most scenes due to the limitation of strimap imaging. In addition, we provide data in different polarizations and bands to study their effects on SAR target characteristics. We simultaneously gather data from satellites and airborne to study the platforms and resolutions.

Table 2 shows the open-source data list. After a year and a half’s effort (from April 2023 to October 2024), we completed program designation, data acquisition and processing, and benchmark construction. We commissioned the Institute of Stealthy Engineering Technology Company in Beijing to complete the data collection and annotation.

3.2 Data acquisition

Here, we present our data acquisition pipeline in terms of imaging, annotation, and product.

Imaging. We use the Unmanned Aerial Vehicle (UAV) platform to carry sensor equipment and collect data. Two antennas acquire quad polarization radar echo in the X and Ku bands. Besides, the Position and Orientation System (POS) device provides the Global Positioning System (GPS) and Inertial

Measurement Unit (IMU) information for motion compensation. After imaging processing, we have slant range complex images. Ground range data is obtained by ground projection based on slant range amplitude images and POS information.

Annotation. We annotate the target types and positions with rectangular box labels according to the optical images and placement positions. Since we focus on individual target characteristics, the targets are placed at a certain distance from each other. Besides our vehicles, other vehicles in the scene are labeled as “other”. After labeling, we acquired the target slices and added a random offset.

Product. We offer data products in two coordinate systems. The distance dimension of the slant range data is the line of sight direction, and we provide original complex data. The ground range images is projected to the ground truth distance and is processed with nonlinear quantization. The corresponding annotation files include basic image information and target, scene, and sensor parameters.

3.3 Professional system

We construct a target taxonomic system to facilitate subsequent extensions and integration with other datasets. Data format and metadata are also discussed, considering the specificity of SAR imaging regarding view, steps, and operating conditions.

Taxonomic system. A taxonomic system is crucial when creating a large-scale fine-grained dataset [10, 29, 67]. Motivated by MSTAR’s military taxonomic system [67] and FUSAR-Ship’s ship taxonomic system [29], our hierarchical taxonomic system (category \rightarrow class \rightarrow type) are based on vehicle’s purpose, structure, size and mass referred to Chinese and European vehicle classification standards [17, 75]. As shown in Fig. 5 (a), we first create 4 main categories based on the vehicle’s

SAR										
Optical										
Class	Mini Car	Mini Car	Medium Car	Medium Car	Large Car	Large Car	Large Car	Compact SUV	Compact SUV	Compact SUV
Brand	Hawtai	Chery	Chery	Buick	Great Wall	Hongqi	Hongqi	Jeep	Mitsubishi	Lincoln
Type	EV160B	QQ3	Arrizo 5	Excelle GT	Voleex C50	CA7180A3E	H5	Patriot	Outlander 2003	MKC
Size (m)	3.52*1.57*1.49	3.56*1.49*1.53	4.57*1.82*1.48	4.58*1.79*1.46	4.67*1.77*1.45	4.79*1.81*1.42	4.98*1.87*1.47	4.42*1.76*1.64	4.55*1.75*1.62	4.55*1.86*1.65
SAR										
Optical										
Class	Medium SUV	Medium SUV	Medium SUV	Small Bus	Small Bus	Small Bus	Small Bus	Medium Bus	Medium Bus	Medium Bus
Brand	Chevrolet	Chang'an	Changfeng Cheetah	Chang'an	Wuling	Buick	Dongfeng	MAXUS	Yangzi	Dongfeng
Type	Blazer 1998	CS75 Plus	CFA6473C	Starlight 4500	Rongguang V	GL8	Forthing Lingzhi	V80	YZK6590XCA	EQ6608LTV
Size (m)	4.65*1.72*1.63	4.67*1.85*1.70	4.80*1.79*1.88	4.39*1.65*1.93	4.41*1.66*1.85	5.10*1.84*1.72	5.13*1.72*1.96	5.70*2.38*2.55	5.95*2.02*2.70	5.99*2.25*2.83
SAR										
Optical										
Class	Large Bus	Pickup	Pickup	Light DT	Light DT	Light DT	Heavy DT	Heavy ST	Heavy ST	Light PV
Brand	Yutong	Great Wall	Huanghai	FAW	Foton	WAW	Dongfeng	Dongfeng	SHACMAN	JAC
Type	ZK6120HY1	Poer	N1	Jaobao T51	BJ1045V9JB5-54	Aochi 1800	Tianjin DFH2200B	Tianjin KR230	DeLong X3000	Junling
Size (m)	11.67*2.50*3.69	5.60*1.88*1.88	5.35*1.79*1.73	3.99*1.51*1.85	5.44*1.92*2.18	5.99*2.20*2.44	7.47*2.35*2.73	9.00*2.55*3.77	16.85*2.49*3.98	5.45*1.91*2.83
SAR										
Optical										
Class	Heavy FT	Heavy FT	Medium TT	Medium TT	Mixer Truck	Forklift	Ambulance	ECV	Road Roller	Shovel Loader
Brand	FAW	SHACMAN	WAW	Dongfeng	CNHTC	Hyundai	JINBEI	Lveco	Changlin	SDLG
Type	J6P	DeLong M3000	Aochi Hongrui	Duolika	HOWO	HLF25 II	SY5033XJH	Proud 2009	8228-5	ZL40F
Size (m)	9.00*2.50*2.85	15.20*3.00*3.65	6.50*1.88*2.30	7.10*2.10*2.40	9.75*2.49*3.95	2.25*1.06*2.13	5.07*1.69*1.93	4.90*2.00*2.50	6.46*2.41*3.33	6.84*2.7*3.24

Fig. 7: Demo images, classes, types, and sizes of forty vehicles in NUDT4MSTAR. Here are the SAR (pseudo-color for better visualization of SAR magnitude images) and corresponding RGB images. As we can see, the obvious difference between the vehicles in the SAR images is the scattering characteristic variation due to size and structure. Therefore, we classify various vehicle types based on their structure and size. Their length, width, and height measurements are listed in meters (m). Besides, it is worth noting that our SAR images are not in the ideal situation where the target is located right in the center of the demo image, just as in the MSTAR dataset, but has a random offset similar to the QinetiQ dataset.

different purposes, such as carrying passengers (car and bus), cargo (truck), and special purposes (special), and passenger and cargo dual-purpose pickup is classified into the truck. Then, we extend them to 21 classes according to the structure, size, and mass differences. For example, cars are based on size and passenger capacity, and trucks depend on length, mass, and special structure. Finally, we collect the 40 vehicle types with size information in Fig. 7. The target classes of SAR vehicle datasets are summarized in Fig. 5 (b). This hierarchical taxonomic system facilitates subsequent standardized acquisition and extensions.

Data format. Due to the unique imaging mechanisms, processing steps, and image properties of SAR, we offer different

levels of products to support the comprehensive study of the impact of imaging steps on recognition problems. We provide magnitude images in the ground range coordinate system with 8-bit and 32-bit uint formats. The magnitude images with 16-bit uint and complex data with 32-bit float in the slant range coordinate system are also available. In subsequent experimental benchmarks, we use 8-bit ground distance magnitude images and 32-bit slant distance complex data. We also perform other processing based on the slant distance data, such as phase gradient autofocus and polarization decomposition, but the current version of this dataset does not include the processed data after these steps. Raw echoes are also stored, but due to

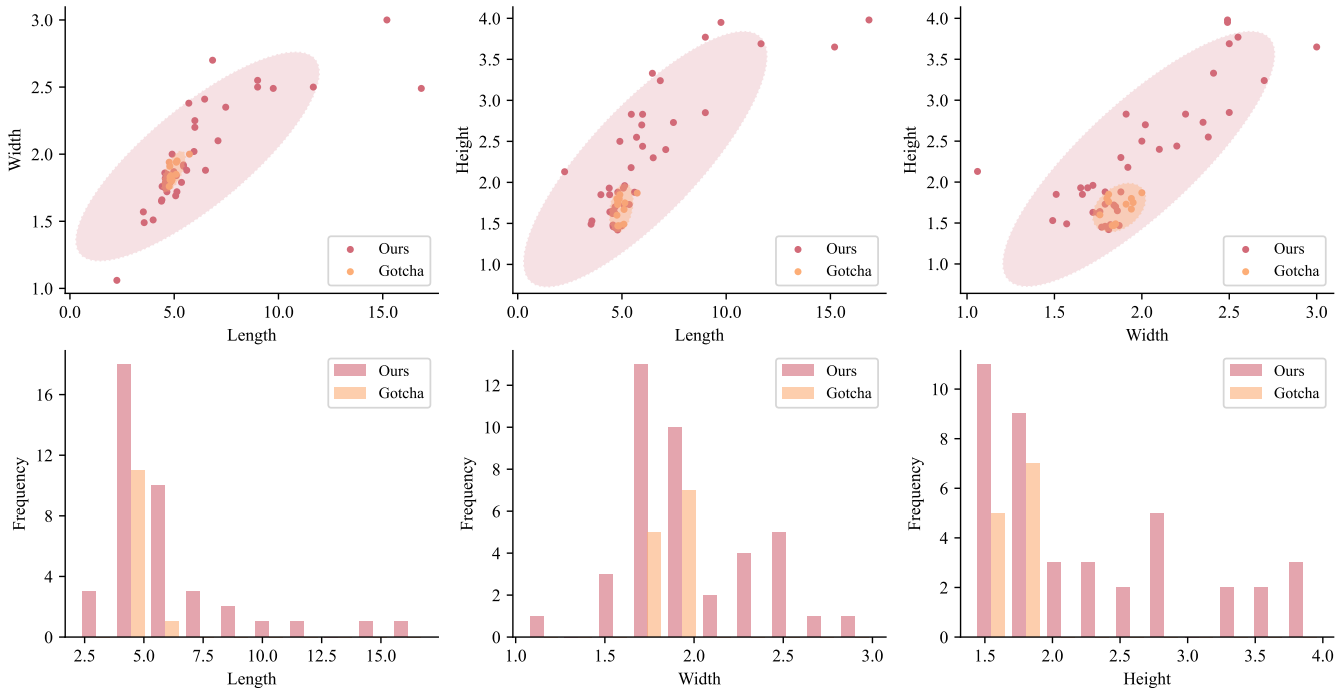


Fig. 8: **Distribution of object size.** Our dataset has a richer object sizes compared to another civilian vehicle dataset (Gotcha). It is clear that the size and ratio of the vehicles are within a certain range due to real-world constraints, such as official regulations and driving requirements, and we will continue to expand the object categories beyond vehicles.

the large storage ($\sim 25\text{TB}$), they will not be available for upload and download. Researchers can contact us to obtain raw echo if needed. We hope these products will help the researchers easily work with our dataset while providing more tractability to explore and discuss specific imaging mechanisms and image properties for SAR recognition applications.

Metadata system. Considering the effects of target, scene, and sensor on SAR images, we add many factors to the annotation to facilitate various recognition methods with metadata. Image information includes basic image sizes and formats. The target attributes include taxonomic systems, target size, and image position. Although we discuss single target characteristics with classification tasks, rectangular boxes also support detection tasks. Sensor parameters have the depression angle, target azimuth angle, band, polarization, and resolution in two dimensions. However, we hope that researchers consider the difficulty and accuracy of obtaining metadata when making full use of them. For example, there is the potential for angular confusion when measuring target azimuths and the potential for vehicle size to change after modifications.

3.4 Statistical Analysis

We now discuss the properties of our dataset and provide some statistics compared with others.

Class distribution. NUDT4MSTAR includes 4 categories, 21 classes and 40 types of vehicles with balanced samples, as shown in Fig. 5. Relative to extant SAR target datasets, our dataset's targets' enhanced diversity and intricacy introduce novel formidable challenges to the SAR target fine-grained recognition research. Moreover, adequate samples guarantee the availability of a substantial array of target classes across experimental settings, facilitating more diverse investigations.

Object size. The length, width, and height of our 40 objects are listed in Fig. 7, and we can see that they have various structures, different sizes, and similar size ratios in Fig. 8.

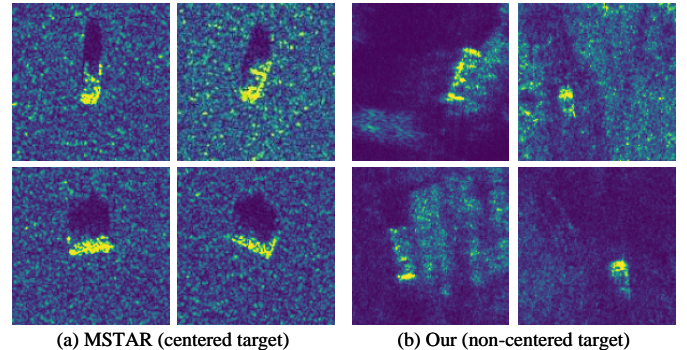


Fig. 9: **Non-centered target slices.** We apply the non-centered target setting following the QinetiQ dataset to increase detection difficulty.

Compared to another civilian vehicle dataset (Gotcha), our dataset has a wider range of target classes and size distribution.

Reference target. Besides deploying corner reflectors for resolution measurements, we produce and place a reference target of multiple geometries as the "SLICY" target in the MSTAR dataset for scattering issues of a standard geometry.

Other vehicle targets. Other vehicle targets in the scene are also labeled for the potential detection task in large remote images. However, this dataset mainly discusses the scattering properties of individual targets. These interfering vehicles can be used as part of a future rejection issue.

Non-centered location. Most SAR target datasets place the target in the image center or contain only the target region, but the QinetiQ dataset uses a non-centered setting. Since remote sensing differs from the human eye view, which customarily centers the object of interest, the overhead view requires searching targets with more interference. As shown in Fig. 9, we randomly added position offsets to increase the recognition difficulty with detecting non-centered target locations.

Occlusion in scenes. Previous vehicle datasets focus on

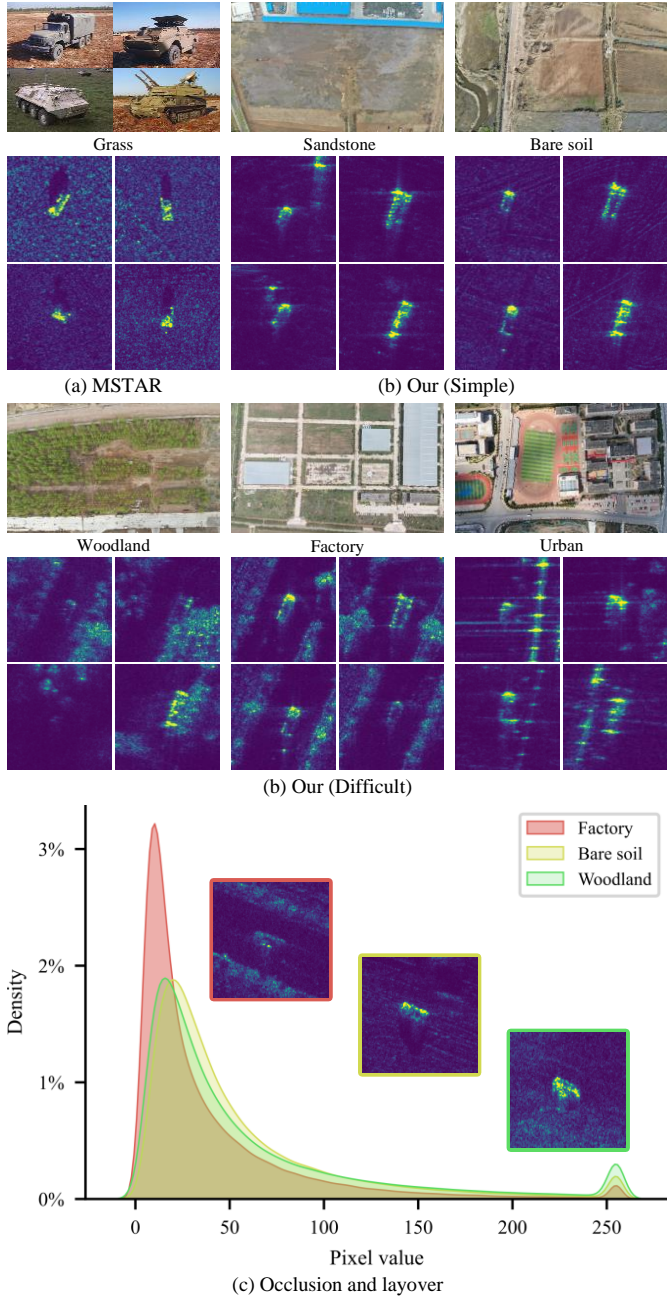


Fig. 10: **Influence of different scenes on target characteristics in SAR images.** Most current SAR target classification datasets are collected in simple scenes, e.g., (a) MSTAR is collected in a flat grass scene with a clean background and pseudo-correlation between target and background. While (b) our NUDT4MSTAR samples are collected under different positions in various scenes. In Fig. (b), it is clear that the same target under the same imaging angle has obvious signature changes due to different scenes. For example, other objects higher up in front of and behind the target can create occlusions and layovers, reducing reflected energy and increasing non-target scattering. Besides, the target shadow in difficult scenes is not as obvious as the MSTAR data. (c) **Occlusion and layover.** Compared to the bare soil scene without interfering objects, the factory and woodland scenarios indicate occlusion and layover. Shadows from interfering objects in the former may obscure targets, while trees in the latter are likely to increase non-target scattering. Due to occlusion and layover are complex results of a combination of target, interference, and imaging geometry, we illustrate this problem with a single target demo. These statistics are from an SUV Chang'an CSCS75 Plus (Vehicle 12) at different image angles in the 3 scenes's ground range images.

target characteristics with simple scenes, and we collect samples from different scenes with the same target and angle. Fig. 10 shows their different influences with occlusions and layovers in different scene regions. The shadow of buildings and roadside trees in the factory may obscure targets and reduce target scattering, and the nearby trees in woodland have more obvious

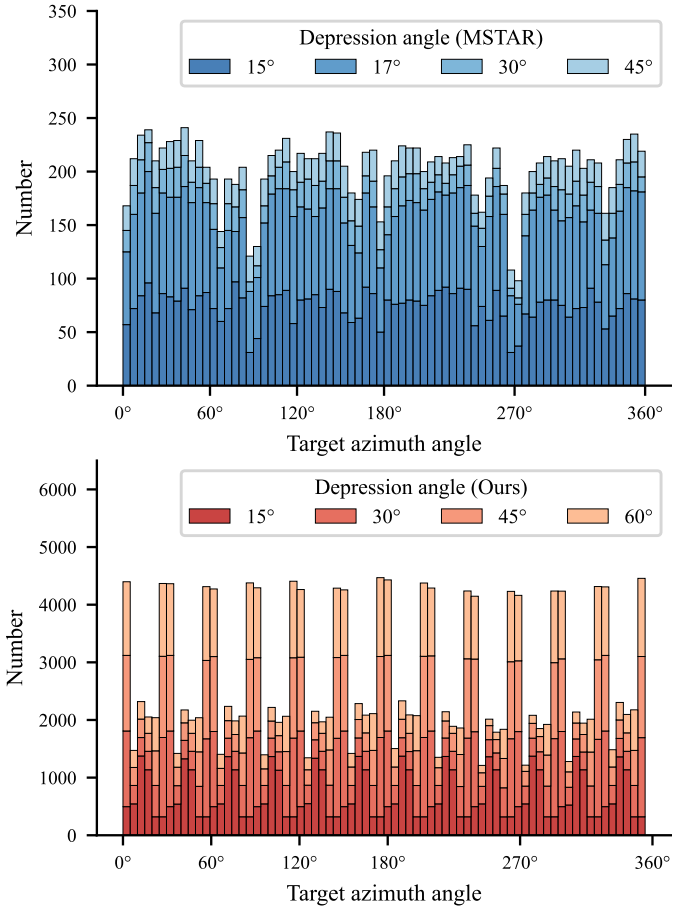


Fig. 11: **Target azimuth angle distribution of (a) MSTAR and (b) NUDT4MSTAR.** Compared to the MSTAR dataset, which has depression angles mainly publicized at 17° and 15° with incomplete angles for most target classes, our NUDT4MSTAR dataset provides balance and comprehensive angles for all targets. However, the sampling interval of target angles is sparser due to strip imaging.

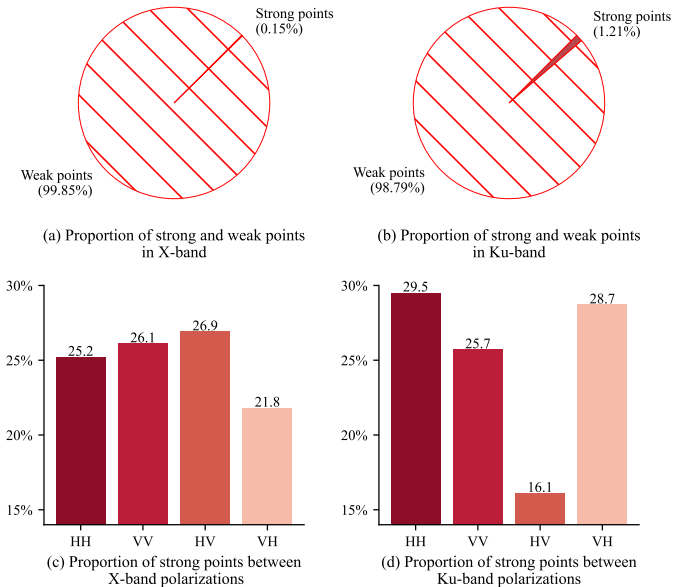


Fig. 12: **Ratio of strong and weak points in different bands and polarizations.** It can be noticed that the band and polarization can have a statistically significant effect on the target signatures. These statistical data are the target region inside the vehicle's rectangular box of sandstone scenes. Points with pixel values greater than or equal to 128 are treated as strong scattering points for 8-bit ground range images.

occlusion and increase non-target scattering.

Imaging angle. Different imaging angles affect the target

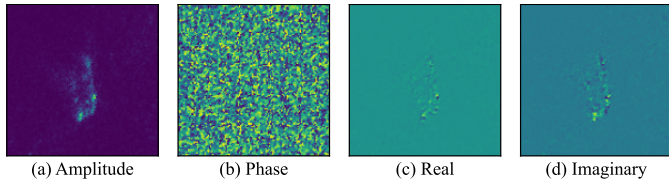


Fig. 13: **Complex data.** Here is a data example of Vehicle 5 (Great Wall Voleex C50).

scattering characteristics, and the imaging geometry relationship can change the interference in the scene. Our dataset has various imaging angles with balance distribution in different depression angles, as shown in Fig. 11. However, the sampling interval of target azimuth angles is not equally dense in different scenes due to the limitation of stripmap imaging and cost problems.

Band and polarization. Table 1 shows most vehicle datasets with the MSTAR dataset’s X-band and HH polarization settings. However, Fig. 12 demonstrates that this setting is not the only one to consider, as band and polarization have a noticeable effect on target scattering. We provide two bands and quad polarization to support discussing these sensor parameters.

Complex data. Feature extraction based on complex data is a hot research concern, so we provide complex data in slant distance coordinates stored in .mat format as Fig. 13 shown.

Number of image bits. RGB images are stored in 8-bit format, whereas SAR images have a larger range of digital data values. Therefore, we provide different bit formats to investigate quantification for enhancing weaker target scattering points.

Cross-platform problem. We collect a small amount of satellite data synchronously under the same scenes and targets to investigate the difficulty of recognition across platforms.

Quality control. To ensure high-quality data, we considered challenges such as target and site hire, airspace applications, weather conditions, and data checking. Eight people completed the data acquisition over six months. In addition, 14 labelers and two inspectors carried out the data annotation over about four months. The entire project cost about CNY 1.45 million.

3.5 Dataset value

Based on the diversity of target categories, scenes, imaging conditions, and data format with detailed annotation, we recommend that this dataset be used for SAR target recognition studies in the following areas.

Robustness recognition. Our data has diverse acquisition conditions, and each image is labeled with specific information. Therefore, we can discuss in detail the robustness of the SAR recognition algorithms when the acquisition conditions (*e.g.*, scene, and sensor) vary between the training and test sets. If we consider data from different acquisition conditions as domains, the training set can include multiple domains to learn domain invariant features, *i.e.*, the domain generalization [99].

Few-shot learning. In addition to acquisition condition variations, the problem of small samples due to high costs is also a concern issue. The few-shot setting can be combined with robust recognition, and our dataset’s large number of target types can enrich the task construction of meta-learning [27, 86, 87] settings in existing few-shot learning.

Transfer learning. Our dataset contains a large diversity of samples that can be used to study the transfer problem of the pre-training model with different SAR target datasets. In addition, the large number of samples can further increase the volume

of SAR target samples to advance the study of self-supervised learning [48, 56] and foundation models [6, 46].

Incremental learning. The diversity of our dataset can support the study of domain incremental learning and class incremental learning [77]. The domain incremental learning can improve the algorithm’s robustness with a dynamic process, and class incremental learning can progressively increase the ability to recognize or reject new classes. This incremental capability is required for SAR ATR systems facing open environments.

Physical deep learning. SAR images have unique properties, such as complex phase and polarization. Our dataset provides a variety of data formats that can support recognition studies based on these unique characteristics rather than relying only on quantified SAR magnitude images. In addition, detailed metadata can also provide more gains for SAR ATR.

We encourage researchers to propose new experimental settings and research issues based on this dataset. *Don’t hesitate to contact us if you get new ideas.*

4 BENCHMARKS

We consider 7 experimental settings with 2 data formats as classification and detection benchmarks for the NUDT4MSTAR dataset in Table 3. These experimental settings include 2 SOC settings sampled from similar distributions and 5 EOC settings with obvious distribution shifts. The data formats are magnitude images in the ground range coordinate system and complex images in the slant range coordinate system.

In conclusion, we evaluate our benchmarks under 7 experimental settings and 15 recognition methods with classification and detection tasks based on magnitude images and classification tasks based on complex images. These experiments provide valuable insights and huge potential into recognizing SAR target characteristics under different imaging conditions and fine-grained classes. Our dataset is sufficient to give a new challenging benchmark to advance SAR target recognition technology. We also welcome researchers to contact us to construct richer experimental benchmarks from original data and publish them with your clear insights.

4.1 Experimental settings

Here, we describe the experimental settings in Table 3, including 2 SOC settings sampled from similar distributions and 5 EOC settings with obvious condition and distribution shifts.

SOC and EOC settings. SOC settings are those where the training and test sets have similar imaging conditions, and we have SOC-40 and SOC-50 settings. SOC-40 is created from a random data sample with a 7:3 training-to-test ratio. SOC-50 randomly selects data with a similar amount of MSTAR ten classes, and we combine our dataset with MSTAR. EOC settings are those where there is a significant domain shift between the training set and the test set, such as variation in imaging conditions and target state. For EOC-Scene, we use simple scenes (sandstone and bare soil) as the training set and complex scenes (urban, factory, and woodland) with occlusion as the test set. EOC-Depression is the training set with a 15° depression angle and the test set with 30°, 45° and 60°. EOC-Azimuth means that training has limited target azimuth angles within 0°~60°, and the test has other angles. Imaging angle and geometry variation can change target signatures and background clutter. EOC-band and EOC-polarization are designed to test the effect of different bands and change from HH-polarization to other

TABLE 3: **SOC and EOC settings of NUDT4MSTAR.** The imaging conditions in SOC are similar, while EOC considers variations in a single imaging condition. Simple scenes are sandstone and bare soil, and complex scenes are urban, factory, and woodland. The separate labeling of the ground distance and slant distance images results in their numbers of annotations not being strictly corresponding. # Types.: Number of object types. Dep.: Depression angle. Azi.: Target azimuth angle. Pol.: Polarization. # Img. (Ground): Number of images in ground range. # Img. (Slant): Number of images in slant range.

Setting	Set	# Types	Scene	Dep.	Azi.	Band	Pol.	# Img. (Ground)	# Img. (Slant)
SOC-40	train	40	all	15, 30, 45, 60	0~360	X & Ku	quad	68,091	67,780
	Test	40	all	15, 30, 45, 60	0~360	X & Ku	quad	29,284	29,169
SOC-50	train	50	all	15, 17, 30, 45, 60	0~360	X & Ku	quad	18,071	18,071
	test	50	all	15, 30, 45, 60	0~360	X & Ku	quad	17,603	17,613
EOC-Scene	train	40	simple	15, 30, 45, 60	0~360	X & Ku	quad	19,584	19,584
	test	40	difficult	15, 30, 45, 60	0~360	X & Ku	quad	77,791	77,365
EOC-Depression	train	40	all	15	0~360	X & Ku	quad	24,361	22,206
	test	40	all	30, 45, 60	0~360	X & Ku	quad	73,014	74,743
EOC-Azimuth	train	40	all	15, 30, 45, 60	0~60	X & Ku	quad	18,636	18,592
	test	40	all	15, 30, 45, 60	60~360	X & Ku	quad	78,739	78,357
EOC-Band	train	40	except city	15, 30, 45, 60	0~360	X	quad	27,711	27,653
	test	40	except city	15, 30, 45, 60	0~360	Ku	quad	27,763	27,732
EOC-Polarization	train	40	all	15, 30, 45, 60	0~360	X & Ku	HH	24,361	24,246
	test	40	all	15, 30, 45, 60	0~360	X & Ku	other	73,014	72,703

polarizations on recognition, respectively. We do not consider some experimental settings that added simulation perturbations, such as random/Gaussian noise and simulation occlusions.

Compared methods. We select classical or recent open-source work in computer vision and SAR target recognition, in addition to recently proposed methods from our laboratory. For classification, we have chosen 6 computer vision methods (VGG16 [69], ResNet18 [26], ResNet34 [26], ConvNeXt [57], ViT [14], and HiViT [96]) and 4 SAR ATR methods (HDANet [50], SARATR-X [46, 48], MS-CVNets [91], and LDSF [88]). MS-CVNets and LDSF are complex images methods others are magnitude methods. VGG16, ResNet18, ResNet34, ConvNeXt, ViT, HiViT, and SARATR-X all use the pre-training weights. For detection, we have chosen 4 computer vision methods (Faster RCNN [66], CenterNet [100], YOLOv8 [36], and YOLOv10 [79]) and 2 SAR ATR methods (DiffDet4SAR [98], and SARATR-X [46, 48]). These methods are based on magnitude images. Because of the long-term dataset construction process, we will keep updating the dataset homepage with new experimental settings and method results.

Transfer learning. To show that this dataset can improve the model’s performance for SAR target feature extraction, we perform training on SOC-40 according to Table 4, and the weights are used for other SAR target classification datasets as initialization for fine-tuning. Fine-tuning parameter settings follow our previous paper [48], and the baseline is the weight of ImageNet supervised pre-training for these models.

4.2 Results and analyses

Here, we present the results of our classification, detection, and transfer learning tasks.

Classification. From different methods in Table 4, we note that deep learning methods can achieve high performance in SAR fine-grained classification, such as the recent methods ConvNeXt and SARATR-X in SOC-40. Methods based on complex images, such as MS-CVNet and LDSF, better distinguish between targets and clutter in EOC-Scene. The model recognition performance and robustness of the latest 2020s CNN architecture

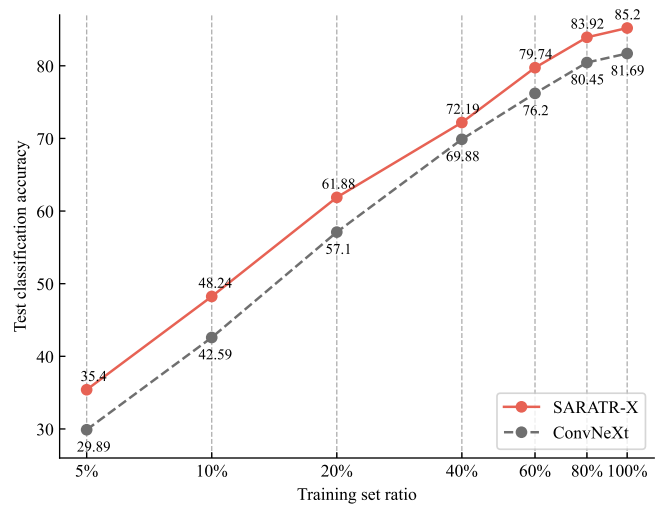


Fig. 14: **Results under SOC-50 with different training set ratio.** We find a linear trend decreasing test set accuracy as training decreases on a logarithmic scale.

ConvNeXt are superior to the previous CNN models. ConvNeXt is more robust under EOC-Depression than other methods, and ViT is insensitive to azimuthal angle change. Our previously proposed method, HDANet, improves the attention mechanism and uses a segmentation task so it can be used in different scenarios. In addition, our proposed LDSF introduces a scattering graph structure that effectively improves the discrimination of targets and clutter. SARATR-X is a pre-trained self-supervised learning model on SAR with the HiViT architecture, and its performance is significantly improved compared to HiViT. Besides, the Transformer models are trained with some low-layer weights frozen, as we found that the full update tends to lead to overfitting.

The different experimental settings in Table 4 show that there are still great challenges in SAR target recognition. As the number of fine-grained classes increased, previous methods were no longer able to achieve nearly 99% accuracy on MSTAR’s SOC. SOC-50 is closer to the actual situation, as we are unlikely

TABLE 4: **Classification results.** We use accuracy as a metric, *i.e.*, the number of correctly classified samples in proportion to the total number of samples. Gray color methods use complex images, and magnitude image methods are sorted by network architecture, such as CNN and Transformer. **Bolded** text indicates the best result, while underlined text is the next best result.

Setting	VGG16 [69]	HDANet [50]	ResNet18 [26]	ResNet34 [26]	ConvNeXt [57]	ViT [14]	HiViT [96]	SARATR-X [46, 48]	MS-CVNet [91]	LDSF [88]
SOC-40	88.8	89.1	90.6	91.7	<u>96.0</u>	76.4	86.8	96.4	80.9	88.2
SOC-50	72.9	63.7	71.2	72.9	<u>81.6</u>	59.2	68.0	85.2	55.2	65.7
EOC-Scene	21.6	33.6	16.1	18.0	16.5	12.9	15.8	19.5	26.1	29.7
– (city)	22.7	33.7	18.1	18.9	17.9	11.6	13.9	20.4	26.1	32.7
– (factory)	20.5	34.3	13.7	16.8	14.4	15.3	17.8	18.4	25.6	30.1
– (woodland)	6.8	27.6	4.2	5.4	4.2	1.97	3.8	2.7	20.2	26.3
EOC-Depression	33.2	32.9	33.9	37.2	43.1	30.4	31.4	<u>39.9</u>	21.8	28.3
– (30)	52.4	54.0	52.2	55.9	63.2	43.7	47.3	<u>58.1</u>	39.2	46.5
– (45)	33.5	32.7	34.2	38.3	45.1	31.0	32.0	<u>41.2</u>	19.2	25.9
– (60)	14.0	12.3	15.4	17.4	21.3	16.7	15.0	<u>20.5</u>	8.1	12.7
EOC-Azimuth	15.7	16.4	14.9	16.5	21.1	29.0	22.8	<u>26.4</u>	19.0	22.5
– (60)	20.7	19.4	18.0	22.1	26.2	34.4	27.2	<u>28.9</u>	26.8	31.0
– (120)	8.2	9.5	8.3	8.5	13.5	26.4	14.2	<u>22.8</u>	13.2	15.6
– (180)	17.6	17.9	16.4	17.4	19.9	20.8	<u>22.2</u>	23.0	16.9	19.7
– (240)	7.11	7.0	7.4	7.9	10.6	20.3	11.1	<u>12.3</u>	10.9	12.6
– (300)	26.0	30.4	25.5	27.5	36.6	<u>44.4</u>	40.9	46.7	28.7	33.7
EOC-Band	78.8	79.5	83.1	83.8	<u>88.4</u>	65.7	70.7	89.2	63.7	60.9
– inverse	74.5	79.8	76.1	79.0	<u>84.6</u>	62.3	78.4	89.1	60.9	64.2
EOC-Polarization	72.5	63.1	71.4	70.5	<u>83.1</u>	53.6	67.1	84.6	49.0	55.1
– VV	72.4	63.0	72.9	72.1	<u>84.4</u>	55.2	69.1	87.5	52.0	63.4
– HV	72.3	62.7	70.2	69.4	<u>82.4</u>	52.4	65.9	83.1	45.8	49.0
– VH	72.8	63.5	71.0	70.0	<u>82.7</u>	55.1	66.5	83.3	46.1	52.8

to obtain a large number of target samples under different conditions. The test set accuracy tends to decrease linearly as the training samples are reduced on a logarithmic scale in Fig 14. In the difficult scene of EOC-Scene, deep learning encounters great challenges, especially in the background clutter interference inside the trees inside the woodland. The significant deterioration in accuracy indicates that deep learning models trained on simple backgrounds have difficulty distinguishing between targets and complex background clutter. The use of complex information or the inclusion of auxiliary tasks such as segmentation during training can enhance the recognition ability, but the alteration of target features due to background clutter interference is still a difficult challenge. We observe a significant decrease using the complex data compared to the magnitude data under angles and sensor parameter variations. These results are because the complex phase is more sensitive to these parameters' transformations, and the magnitude of the data is additionally preprocessed to enhance the image's visual quality. Changes in imaging angle have a greater impact on target characteristics than band and polarization, especially large depression and azimuth angle changes. Different imaging angles lead to variations in target and background clutter, as well as different occlusions and scattering resulting from changes in imaging geometry. We have not found a good method to deal with the above scene and angle changes. The shift in target features due to band and polarization can be solved very effectively by ConvNeXt and SARATR-X. However, due to cost issues, we have not discussed the effect of different platform resolutions on recognition in the current version, which is another important issue.

Detection. As illustrated in Table 5, we find that the two-stage approach (Faster RCNN, DiffDet4SAR, and SARATR-X)

TABLE 5: **Detection results.** We use mAP50 [55] as a metric, *i.e.*, the average precision at IoU 0.5 because the horizontal bounding box does not exactly fit the contours of the different targets. **Bolded** text indicates the best result, while underlined text is the next best result.

Setting	CenterNet [100]	YOLOv8 [36]	YOLOv10 [79]	Faster RCNN [66]	DiffDet4SAR [98]	SARATR-X [46, 48]
SOC-40	83.5	86.1	<u>91.7</u>	88.3	90.9	95.5
SOC-50	74.7	64.4	63.5	65.0	<u>76.1</u>	79.6
EOC-Scene	30.2	26.2	21.5	<u>35.5</u>	37.2	20.4
– (city)	37.8	30.8	24.8	<u>42.6</u>	45.9	18.1
– (factory)	27.1	24.3	20.3	<u>32.9</u>	35.2	24.1
– (woodland)	23.8	25.1	20.0	<u>30.7</u>	32.8	25.2
EOC-Depression	<u>33.5</u>	22.7	22.3	29.0	31.0	33.3
– (30)	57.3	42.9	42.5	50.1	52.1	55.4
– (45)	<u>34.2</u>	21.4	21.6	27.7	30.1	35.0
– (60)	8.1	4.4	4.1	6.4	<u>8.2</u>	9.9
EOC-Azimuth	24.5	18.1	19.2	<u>26.9</u>	28.7	22.9
– (60)	21.4	15.9	18.6	<u>26.8</u>	28.9	20.5
– (120)	20.0	13.0	14.3	20.8	<u>22.1</u>	22.3
– (180)	18.7	15.0	14.1	<u>19.0</u>	20.1	18.6
– (240)	14.9	10.4	11.4	<u>18.0</u>	19.0	14.0
– (300)	56.0	44.6	44.7	<u>57.9</u>	60.1	46.7
EOC-Band	69.1	72.4	74.5	72.9	<u>75.1</u>	87.5
– inverse	<u>75.9</u>	75.2	72.1	69.5	73.8	83.7
EOC-Polarization	74.8	56.0	59.2	58.3	61.2	75.3
– VV	<u>75.6</u>	56.9	62.4	57.9	60.4	77.4
– HV	74.3	55.3	57.6	59.0	62.1	<u>73.9</u>
– VH	<u>75.1</u>	56.4	58.3	58.5	61.0	74.8

has better robustness than the single-stage approach (CenterNet, YOLOv8, and YOLOv10) under most EOC conditions. In particular, CenterNet models the target center using a Gaussian kernel, demonstrating superior detection capabilities under EOC-Depression and EOC-Polarization conditions. However,

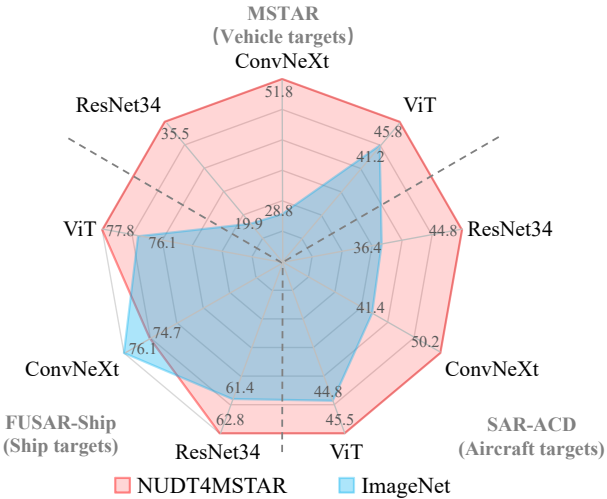


Fig. 15: **Transfer learning results.** We report the 5-shot fine-tuning performance of transfer learning on three SAR target classification datasets after NUDT4MSTAR training. The results show that our dataset has a good effect on ground target datasets such as vehicles and aircraft, but the effect is insignificant for sea targets.

YOLO series methods, which rely on fixed grid partitioning and coordinate regression, exhibit limitations in detection performance under EOC conditions. In contrast, our proposed DiffDet4SAR, a diffusion model-based detection framework, consistently outperforms other algorithms in EOC-SCENE and EOC-Azimuth scenarios. This advantage stems from the robust denoising box structure, which enhances target location accuracy, and the use of central difference convolution to amplify target saliency. The foundation model SARATR-X, based on self-supervised learning with SAR images, performs well for fine-grained recognition and most of the EOC conditions, but the performance for scene and angle changes needs to be improved.

Compared with the classification task, the detection task can effectively distinguish between target and background clutter, especially for target discovery in complex scenes such as woodlands. However, most of the detection performance is slightly lower than the classification performance due to the SAR image quality issues that result in noisy labels and rectangular box offsets. Besides, our fine-grained detection tasks, encompassing both accurate localization and precise classification, are inherently more complex than single precise classification tasks, necessitating advanced model architectures and sophisticated algorithm designs. Furthermore, although we changed the target position, such adjustments are not performed frequently due to acquisition time and cost constraints. Similarly, there is still much scope for improvement in robustness under scene and imaging angle variations.

Transfer learning. Fig 15 shows how our dataset can help different models benefit from feature learning and be used for target recognition in other datasets. We use Table's SOC-40 trained model weights as initializations on other target datasets with 5-shot sample experiments [48]. The fine-tuning results show that similar ground target-type datasets, such as vehicles and airplanes, would greatly benefit from training on our data. However, the transfer effect is not obvious for the ship target class dataset in the sea scene.

4.3 Discussion

Researchers have pursued realizing a stable and efficient SAR ATR recognition system, but previous vehicle benchmark

datasets have not provided difficult challenges. Our results show that current state-of-the-art methods still face many robustness and small sample difficulties. Robust feature extraction under different imaging conditions and scenes is still a worthy research problem. It is also important to efficiently use a small number of labeled samples and mine complex and polarization information. Moreover, there is no single method that can handle different perturbation conditions, demonstrating the complexity of stable SAR ATR. Of course, building a large-scale dataset and advancing SAR ATR technology is a long-term process. In a data-driven approach dominant in the 2020s, a large-scale dataset will help to extract stabilizing features and be effective in many other datasets and tasks. Based on the results, we discuss several potential directions for the future development of ATR systems.

Robustness under different conditions. As Table 4 and 5 show, the variations in imaging conditions present a significant challenge for recognition. This variability in the domain distribution requires the extraction of stable invariant target features under different conditions.

Efficient utilization of samples. Due to the difficulty of acquiring and labeling SAR images, it is unlikely that the sample size will reach the same size as the visible light dataset. Therefore, it is important to improve learning efficiency by utilizing a small number of samples in Fig 14.

Incorporation with multi-dimensional information. Using magnitude images alone loses many SAR image attributes, such as complex information that can effectively distinguish between targets and clutter in Table 4. Therefore, auxiliary information such as complex, polarization, and angle can be introduced in SAR ATR, but increasing the dimensionality of the information may increase the instability and complexity of the features.

Fast incremental learning capability. Because of the open and dynamic world, real ATR systems face constantly changing imaging conditions and target types. They need to effectively recognize anomalies and update their capabilities in response to variations. This data provides a rich set of target types and imaging conditions that can be used to explore this possibility.

Subsequently, we plan to construct a different resolution version and paired polarization data. We will continue to expand the scenes and target classes by combining satellite data with a semi-automated and low-cost method.

5 CONCLUSION

A large-scale fine-grained SAR vehicle dataset and benchmark, named **NUDT4MSTAR**, has been established in this paper. It contains various target types, scene variations, and imaging conditions and is 10 times the size of previous datasets of the same type. Our benchmark of 7 experiment settings and 15 methods result show that stable and efficient SAR ATR recognition method are still challengeable. It will advance diverse issue explorations and SAR ATR techniques with large-scale data. In the future, we will continue to contribute to the SAR target datasets, and we welcome researchers to contact us to jointly promote the progress of the SAR ATR field.

REFERENCES

- [1] Ali Ahmadibeni, Leila Borooshak, Brandon Jones, and Amir Shirkhodaie. Aerial and ground vehicles synthetic SAR dataset generation for automatic target recognition. In *Proc. SPIE Conf. Algorithms SAR Imagery*, volume 11393, pages 96–107, 2020.
- [2] Air Force Research Laboratory. The air force moving and stationary target recognition database. <https://www.sdms.afrl.af.mil/index.php?collection=mstar>.

[3] Meng Bao, Jie Zhang, Junmin Meng, Xi Zhang, and Haitao Lang. Construction and feature analysis of high resolution SAR ship sample set (in chinese). *Chin. J. Radio Sci.*, 34(6):789–797, 2019.

[4] Favyen Bastani, Piper Wolters, Ritwik Gupta, Joe Ferdinando, and Aniruddha Kembhavi. SatlasPretrain: A large-scale dataset for remote sensing image understanding. In *Proc. IEEE Int. J. Comput. Vis. (ICCV)*, pages 16772–16782, 2023.

[5] Carole Belloni, Alessio Balleri, Nabil Aouf, Thomas Merlet, and Jean-Marc Le Caillec. SAR image dataset of military ground targets with multiple poses for ATR. In *Proc. Target Background Signatures III*, volume 10432, pages 218–225, 2017.

[6] Rishi Bommasani, Drew A Hudson, Ehsan Adeli, Russ Altman, Simran Arora, Sydney von Arx, Michael S Bernstein, Jeannette Bohg, Antoine Bosselut, Emma Brunskill, et al. On the opportunities and risks of foundation models. *arXiv preprint*, 2021.

[7] Jiacheng Chen, Xu Zhang, Haipeng Wang, and Feng Xu. A reinforcement learning framework for scattering feature extraction and SAR image interpretation. *IEEE Trans. Geosci. Remote Sens.*, 62:1–14, 2024.

[8] Sizhe Chen, Haipeng Wang, Feng Xu, and Yaqiu Jin. Target classification using the deep convolutional networks for SAR images. *IEEE Trans. Geosci. Remote Sens.*, 54(8):4806–4817, 2016.

[9] Mihai Datcu, Zhongling Huang, Andrei Anghel, Juanping Zhao, and Remus Cacoveanu. Explainable, physics-aware, trustworthy artificial intelligence: A paradigm shift for synthetic aperture radar. *IEEE Geosci. Remote Sens. Mag.*, 11(1):8–25, 2023.

[10] Jia Deng, Wei Dong, Richard Socher, Li-Jia Li, Kai Li, and Li Fei-Fei. ImageNet: A large-scale hierarchical image database. In *Proc. IEEE Comput. Soc. Conf. Comput. Vis. Pattern Recognit. (CVPR)*, pages 248–255. Ieee, 2009.

[11] Baiyuan Ding, Gongjian Wen, Xiaohong Huang, Conghui Ma, and Xiaoliang Yang. Target recognition in synthetic aperture radar images via matching of attributed scattering centers. *IEEE J. Sel. Top. Appl. Earth Obs. Remote Sens.*, 10(7):3334–3347, 2017.

[12] Jun Ding, Bo Chen, Hongwei Liu, and Mengyuan Huang. Convolutional neural network with data augmentation for SAR target recognition. *IEEE Geosci. Remote Sens. Lett.*, 13(3):364–368, 2016.

[13] Ganggang Dong, Hongwei Liu, and Jocelyn Chanussot. Keypoint-based local descriptors for target recognition in SAR images: A comparative analysis. *IEEE Geosci. Remote Sens. Mag.*, 9(1):139–166, 2020.

[14] Alexey Dosovitskiy, Lucas Beyer, Alexander Kolesnikov, Dirk Weissenborn, Xiaohua Zhai, Thomas Unterthiner, Mostafa Dehghani, Matthias Minderer, Georg Heigold, Sylvain Gelly, et al. An image is worth 16x16 words: Transformers for image recognition at scale. *arXiv preprint*, 2020.

[15] Kerry E Dungan, Joshua N Ash, John W Nehrbass, Jason T Parker, LeRoy A Gorham, and Steven M Scarborough. Wide angle SAR data for target discrimination research. In *Proc. SPIE Conf. Algorithms SAR Imagery*, volume 8394, pages 181–193, 2012.

[16] Kerry E Dungan, Christian Austin, John Nehrbass, and Lee C Potter. Civilian vehicle radar data domes. In *Proc. SPIE Conf. Algorithms SAR Imagery*, volume 7699, pages 242–253, 2010.

[17] European Commission. EU classification of vehicle types. <https://alternative-fuels-observatory.ec.europa.eu/general-information/vehicle-types>.

[18] Jinxiang Fan and Jia Liu. The challenges and some thinking for the intelligentization of precision guidance ATR. In *Artif. Intell. Mach. Learn. Def. Appl.*, volume 11169, pages 209–217. SPIE, 2019.

[19] Sijia Feng, Kefeng Ji, Fulai Wang, Linbin Zhang, Xiaojie Ma, and Gangyao Kuang. Electromagnetic scattering feature (ESF) module embedded network based on ASC model for robust and interpretable SAR ATR. *IEEE Trans. Geosci. Remote Sens.*, 60:1–15, 2022.

[20] XU Feng and JIN Yaqiu. Microwave vision and intelligent perception of radar imagery (in chinese). *J. Radars*, 13(2):285–306, 2024.

[21] Kun Fu, Tengfei Zhang, Yue Zhang, Zhirui Wang, and Xian Sun. Few-shot sar target classification via metalearning. *IEEE Trans. Geosci. Remote Sens.*, 60:1–14, 2022.

[22] Valerio Gagliardi, Fabio Tosti, Luca Bianchini Ciampoli, Maria Libera Battagliere, Luigi D’Amato, Amir M Alani, and Andrea Benedetto. Satellite remote sensing and non-destructive testing methods for transport infrastructure monitoring: Advances, challenges and perspectives. *Remote Sens.*, 15(2):418, 2023.

[23] Gui Gao. An improved scheme for target discrimination in high-resolution SAR images. *IEEE Trans. Geosci. Remote Sens.*, 49(1):277–294, 2010.

[24] Zhe Geng, Ying Xu, Bei-Ning Wang, Xiang Yu, Dai-Yin Zhu, and Gong Zhang. Target recognition in SAR images by deep learning with training data augmentation. *Sensors*, 23(2):941, 2023.

[25] Yue Guo, Shiqi Chen, Ronghui Zhan, Wei Wang, and Jun Zhang. LSD-YOLO: A lightweight YOLO algorithm for multi-scale SAR ship detection. *Remote Sens.*, 14(19):4801, 2022.

[26] Kaiming He, Xiangyu Zhang, Shaoqing Ren, and Jian Sun. Deep residual learning for image recognition. In *Proc. IEEE Comput. Soc. Conf. Comput. Vis. Pattern Recognit. (CVPR)*, pages 770–778, 2016.

[27] Timothy Hospedales, Antreas Antoniou, Paul Micaelli, and Amos Storkey. Meta-learning in neural networks: A survey. *IEEE Trans. Pattern Anal. Mach. Intell.*, 44(9):5149–5169, 2021.

[28] Biao Hou, Bo Ren, Guilin Ju, Huiyan Li, Licheng Jiao, and Jin Zhao. SAR image classification via hierarchical sparse representation and multisize patch features. *IEEE Geosci. Remote Sens. Lett.*, 13(1):33–37, 2015.

[29] Xiyue Hou, Wei Ao, Qian Song, Jian Lai, Haipeng Wang, and Feng Xu. FUSAR-Ship: Building a high-resolution SAR-AIS matchup dataset of Gaofen-3 for ship detection and recognition. *Sci. China Inf. Sci.*, 63:1–19, 2020.

[30] Lanqing Huang, Bin Liu, Boying Li, Weiwei Guo, Wenhao Yu, Zenghui Zhang, and Wenxian Yu. OpenSARShip: A dataset dedicated to Sentinel-1 ship interpretation. *IEEE J. Sel. Top. Appl. Earth Obs. Remote Sens.*, 11(1):195–208, 2018.

[31] Zhongling Huang, Chong Wu, Xiwen Yao, Zhicheng Zhao, Xiankai Huang, and Junwei Han. Physics inspired hybrid attention for SAR target recognition. *ISPRS J. Photogramm. Remote Sens.*, 207:164–174, 2024.

[32] Zhongling Huang, Xiwen Yao, Ying Liu, Cornelius Octavian Dumitru, Mihai Datcu, and Junwei Han. Physically explainable CNN for SAR image classification. *ISPRS J. Photogramm. Remote Sens.*, 190:25–37, 2022.

[33] Katsushi Ikeuchi, Takeshi Shakunaga, Mark D Wheeler, and Taku Yamazaki. Invariant histograms and deformable template matching for SAR target recognition. In *Proc. IEEE Comput. Soc. Conf. Comput. Vis. Pattern Recognit. (CVPR)*, pages 100–105. IEEE, 1996.

[34] Nathan Inkawich. A global model approach to robust few-shot sar automatic target recognition. *IEEE Geosci. Remote Sens. Lett.*, 2023.

[35] Xinhua Jiang, Tianpeng Liu, Yongxiang Liu, Shuanghui Zhang, Huangxing Lin, and Li Liu. An azimuth aware deep reinforcement learning framework for active SAR target recognition. *IEEE J. Sel. Top. Appl. Earth Obs. Remote Sens.*, 2024.

[36] Glenn Jocher, Ayush Chaurasia, and Jing Qiu. Ultralytics YOLO. <https://github.com/ultralytics/ultralytics>, Jan 2023.

[37] Grinnell Jones and Bir Bhanu. Recognition of articulated and occluded objects. *IEEE Trans. Pattern Anal. Mach. Intell.*, 21(7):603–613, 1999.

[38] Odysseas Kechagias-Stamatis and Nabil Aouf. Fusing deep learning and sparse coding for SAR ATR. *IEEE Trans. Aerosp. Electron. Syst.*, 55(2):785–797, 2018.

[39] Odysseas Kechagias-Stamatis and Nabil Aouf. Automatic target recognition on synthetic aperture radar imagery: A survey. *IEEE Aerosp. Electron. Syst. Mag.*, 36(3):56–81, 2021.

[40] Y. Lecun, L. Bottou, Y. Bengio, and P. Haffner. Gradient-based learning applied to document recognition. *Proc. IEEE*, 86(11):2278–2324, 1998.

[41] Benjamin Lewis, Omar DeGuchi, Joseph Sebastian, and John Kaminski. Realistic SAR data augmentation using machine learning techniques. In *Proc. 26th SPIE Conf. Algorithms SAR Imagery*, volume 10987, pages 12–28, 2019.

[42] Benjamin Lewis, Theresa Scarnati, Elizabeth Sudkamp, John Nehrbass, Stephen Rosencrantz, and Edmund Zelnio. A SAR dataset for ATR development: the synthetic and measured paired labeled experiment (SAMPLE). In *Proc. SPIE Conf. Algorithms SAR Imagery*, volume 10987, pages 39–54, 2019.

[43] Chen Li, Lan Du, Yi Li, and Jialun Song. A novel SAR target recognition method combining electromagnetic scattering information and GCN. *IEEE Geosci. Remote Sens. Lett.*, 19:1–5, 2022.

[44] Jianwei Li, Zhentao Yu, Lu Yu, Pu Cheng, Jie Chen, and Cheng Chi. A comprehensive survey on SAR ATR in deep-learning era. *Remote Sens.*, 15(5):1454, 2023.

[45] Tingli Li and Lan Du. SAR automatic target recognition based on attribute scattering center model and discriminative dictionary learning. *IEEE Sens. J.*, 19(12):4598–4611, 2019.

[46] Weijie Li, Wei Yang, Yuenan Hou, Li Liu, Yongxiang Liu, and Xiang Li. SARATR-X: Towards building a foundation model for SAR target recognition. *arXiv preprint*, 2024.

[47] Weijie Li, Wei Yang, Li Liu, Wenpeng Zhang, and Yongxiang Liu. Discovering and explaining the noncausality of deep learning in SAR ATR. *IEEE Geosci. Remote Sens. Lett.*, 20:1–5, 2023.

[48] Weijie Li, Wei Yang, Tianpeng Liu, Yuenan Hou, Yuxuan Li, Zhen Liu, Yongxiang Liu, and Li Liu. Predicting gradient is better: Exploring self-supervised learning for SAR ATR with a joint-embedding predictive architecture. *ISPRS J. Photogramm. Remote Sens.*, 218:326–338, 2024.

[49] Weijie Li, Wei Yang, Yongxiang Liu, and Xiang Li. Research and exploration on the interpretability of deep learning model in radar image (in chinese). *Sci. Sin. Inform.*, 52:1114–1134, 2022.

[50] Weijie Li, Wei Yang, Wengpeng Zhang, Tianpeng Liu, Yongxiang Liu, and Li Liu. Hierarchical disentanglement-alignment network for robust SAR vehicle recognition. *IEEE J. Sel. Top. Appl. Earth Obs. Remote Sens.*, 16:9661–9679, 2023.

[51] Yansheng Li, Linlin Wang, Tingzhu Wang, Xue Yang, Junwei Luo, Qi Wang, Youming Deng, Wenbin Wang, Xian Sun, Haifeng Li, et al. STAR: A first-ever dataset and a large-scale benchmark for scene graph generation in large-size satellite imagery. *arXiv preprint*, 2024.

[52] Yuxuan Li, Xiang Li, Weijie Li, Qibin Hou, Li Liu, Ming-Ming Cheng, and Jian Yang. Sardet-100k: Towards open-source benchmark and toolkit for large-scale sar object detection. *arXiv preprint*, 2024.

[53] Jinrui Liao, Yikui Zhai, Qingsong Wang, Bing Sun, and Vincenzo Piuri. LDCL: Low-confidence discriminant contrastive learning for small-sample SAR ATR. *IEEE Trans. Geosci. Remote Sens.*, 62:1–17, 2024.

[54] Jiaming Liu, Mengdao Xing, Hanwen Yu, and Guangcai Sun. EFTL: Complex convolutional networks with electromagnetic feature transfer learning for SAR target recognition. *IEEE Trans. Geosci. Remote Sens.*, 60:1–11, 2022.

[55] Li Liu, Wanli Ouyang, Xiaogang Wang, Paul Fieguth, Jie Chen, Xinwang Liu, and Matti Pietikäinen. Deep learning for generic object detection: A survey. *Int. J. Comput. Vision*, 128:261–318, 2020.

[56] Xiao Liu, Fanjin Zhang, Zhenyu Hou, Li Mian, Zhaoyu Wang, Jing Zhang, and Jie Tang. Self-supervised learning: Generative or contrastive. *IEEE Trans. Knowl. Data Eng.*, 35(1):857–876, 2021.

[57] Zhuang Liu, Hanzi Mao, Chao-Yuan Wu, Christoph Feichtenhofer, Trevor Darrell, and Saining Xie. A convnet for the 2020s. In *Proc. IEEE Comput. Soc. Conf. Comput. Vis. Pattern Recognit. (CVPR)*, pages 11976–11986, 2022.

[58] Jialin Luo, Yuanzhi Wang, Ziqi Gu, Yide Qiu, Shuaizhen Yao, Fuyun Wang, Chunyan Xu, Wenhua Zhang, Dan Wang, and Zhen Cui. MMM-RS: A multi-modal, multi-GSD, multi-scene remote sensing dataset and benchmark for text-to-image generation. *arXiv preprint*, 2024.

[59] David Malmgren-Hansen, Anders Kusk, Jørgen Dall, Allan Aasbjerg Nielsen, Rasmus Engholm, and Henning Skriver. Improving SAR automatic target recognition models with transfer learning from simulated data. *IEEE Geosci. Remote Sens. Lett.*, 14(9):1484–1488, 2017.

[60] David Malmgren-Hansen, Morten Nobel-J, et al. Convolutional neural networks for SAR image segmentation. In *Proc. IEEE Int. Symp. Signal Process. Inf. Technol.*, pages 231–236, 2015.

[61] Alberto Moreira, Pau Prats-Iraola, Marwan Younis, Gerhard Krieger, Irena Hajnsek, and Konstantinos P Papathanassiou. A tutorial on synthetic aperture radar. *IEEE Geosci. Remote Sens. Mag.*, 1(1):6–43, 2013.

[62] Jifang Pei, Yulin Huang, Weibo Huo, Yin Zhang, Jianyu Yang, and Tat-Soon Yeo. SAR automatic target recognition based on multiview deep learning framework. *IEEE Trans. Geosci. Remote Sens.*, 56(4):2196–2210, 2018.

[63] Lee C Potter and Randolph L Moses. Attributed scattering centers for SAR ATR. *IEEE Trans. Image Process.*, 6(1):79–91, 1997.

[64] Markus Reichstein, Gustau Camps-Valls, Bjorn Stevens, Martin Jung, Joachim Denzler, Nuno Carvalhais, and F Prabhat. Deep learning and process understanding for data-driven earth system science. *Nature*, 566(7743):195–204, 2019.

[65] Haohao Ren, Xuelian Yu, Lin Zou, Yun Zhou, Xuegang Wang, and Lorenzo Bruzzone. Extended convolutional capsule network with application on SAR automatic target recognition. *Signal Process.*, 183:108021, 2021.

[66] Shaoqing Ren, Kaiming He, Ross Girshick, and Jian Sun. Faster R-CNN: Towards real-time object detection with region proposal networks. *IEEE Trans. Pattern Anal. Mach. Intell.*, 39(6):1137–1149, 2016.

[67] Timothy D Ross, Jeff J Bradley, Lannie J Hudson, and Michael P O’connor. SAR ATR: So what’s the problem? An MSTAR perspective. In *Proc. SPIE Conf. Algorithms SAR Imagery*, volume 3721, pages 662–672, 1999.

[68] Rolf Schumacher and Kh Rosenbach. ATR of battlefield targets by SAR classification results using the public MSTAR dataset compared with a dataset by QinetiQ UK. In *Proc. RTO SET Symp. Target Identificat. Recognit. Using RF Syst.*, pages 11–13, 2004.

[69] Karen Simonyan and Andrew Zisserman. Very deep convolutional networks for large-scale image recognition. In *Proc. Int. Conf. Learn. Represent. (ICLR)*, 2015.

[70] Shengli Song, Bin Xu, and Jian Yang. SAR target recognition via supervised discriminative dictionary learning and sparse representation of the SAR-HOG feature. *Remote Sens.*, 8(8):683, 2016.

[71] Marc Spigai, Céline Tison, and Jean-Claude Souyris. Time-frequency analysis in high-resolution SAR imagery. *IEEE Trans. Geosci. Remote Sens.*, 49(7):2699–2711, 2011.

[72] Guang-Cai Sun, Yanbin Liu, Jixiang Xiang, Wenkang Liu, Mengdao Xing, and Jianlai Chen. Spaceborne synthetic aperture radar imaging algorithms: An overview. *IEEE Geosci. Remote Sens. Mag.*, 10(1):161–184, 2021.

[73] Xian Sun, Yixuan Lv, Zhirui Wang, and Kun Fu. SCAN: Scattering characteristics analysis network for few-shot aircraft classification in high-resolution SAR images. *IEEE Trans. Geosci. Remote Sens.*, 60:1–17, 2022.

[74] Xiaobao Tong and Yong Wang. Active multi-view fusion framework for SAR automatic target recognition. *IEEE Trans. Instrum. Meas.*, 2023.

[75] Traffic Management. Road traffic management-types of motor vehicles, GA 802-2019 (in chinese). <http://jjzd.yiyang.gov.cn/uploadfiles/202405/2024052815445075152.pdf>.

[76] Arsenios Tsokas, Maciej Rysz, Panos M Pardalos, and Kathleen Dipple. SAR data applications in earth observation: An overview. *Expert Syst. Appl.*, 205:117342, 2022.

[77] Gido M Van de Ven, Tinne Tuytelaars, and Andreas S Tolias. Three types of incremental learning. *Nat. Mach. Intell.*, 4(12):1185–1197, 2022.

[78] Ashish Vaswani, Noam Shazeer, Niki Parmar, Jakob Uszkoreit, Llion Jones, Aidan N Gomez, Łukasz Kaiser, and Illia Polosukhin. Attention is all you need. In *Proc. Adv. Neural Inf. Process. Syst. (NeurIPS)*, volume 30, 2017.

[79] Ao Wang, Hui Chen, Lihao Liu, Kai Chen, Zijia Lin, Jungong Han, and Guiguang Ding. Yolov10: Real-time end-to-end object detection. *arXiv preprint arXiv:2405.14458*, 2024.

[80] Di Wang, Yongping Song, Junnan Huang, Daoxiang An, and Leping Chen. SAR target classification based on multiscale attention super-class network. *IEEE J. Sel. Top. Appl. Earth Obs. Remote Sens.*, 15:9004–9019, 2022.

[81] Ruyi Wang, Hanqing Zhang, Bing Han, Yueteng Zhang, Jiayi Guo, Wen Hong, Wei Sun, and Wenlong Hu. Multiangle SAR dataset construction of aircraft targets based on angle interpolation simulation (in chinese). *J. Radars*, 11(4):637–651, 2022.

[82] Yanni Wang, Hecheng Jia, Shilei Fu, Huiping Lin, and Feng Xu. Reinforcement learning for SAR target orientation inference with the differentiable SAR renderer. *IEEE Trans. Geosci. Remote Sens.*, pages 1–1, 2024.

[83] Qian-Ru Wei, Cheng-Yu Chen, Mingyi He, and Hong-Mei He. Zero-shot SAR target recognition based on classification assistance. *IEEE Geosci. Remote Sens. Lett.*, 20:1–5, 2023.

[84] ZaiDao Wen, ZhunGa Liu, Shuai Zhang, and Quan Pan. Rotation awareness based self-supervised learning for SAR target recognition with limited training samples. *IEEE Trans. Image Process.*, 30:7266–7279, 2021.

[85] Youming Wu, Yuxi Suo, Qingbiao Meng, Wei Dai, Tiao Miao, Wenchao Zhao, Zhiyuan Yan, Wenhui Diao, Guocun Xie, Qingyang Ke, et al. FAIR-CSAR: A benchmark dataset for fine-grained object detection and recognition based on single look complex SAR images. *IEEE Trans. Geosci. Remote Sens.*, 2024.

[86] Jing-Yuan Xia, Shengxi Li, Jun-Jie Huang, Zhixiong Yang, Imad M. Jaimoukha, and Deniz Gündüz. Metalearning-based alternating minimization algorithm for nonconvex optimization. *IEEE Trans. Neural Networks Learn. Syst.*, 34(9):5366–5380, 2023.

[87] Jingyuan Xia, Zhixiong Yang, Shengxi Li, Shuanghui Zhang, Yaowen Fu, Deniz Gündüz, and Xiang Li. Blind super-resolution via meta-learning and markov chain monte carlo simulation. *IEEE Trans. Pattern Anal. Mach. Intell.*, 46(12):8139–8156, 2024.

[88] Xuying Xiong, Xinyu Zhang, Weidong Jiang, Tianpeng Liu, Yongxiang Liu, and Li Liu. Lightweight dual-stream SAR-ATR framework based on an attention mechanism-guided heterogeneous graph network. *IEEE J. Sel. Top. Appl. Earth Obs. Remote Sens.*, pages 1–22, 2024.

[89] Haodong Yang, Xinyue Kang, Long Liu, Yujiang Liu, and Zhongling Huang. SAR-HUB: Pre-training, fine-tuning, and explaining. *Remote Sens.*, 15(23):5534, 2023.

[90] Xinyi Ying, Chao Xiao, Ruojing Li, Xu He, Boyang Li, Zhaoxu Li, Yingqian Wang, Mingyuan Hu, Qingyu Xu, Zaiping Lin, Miao Li, Shilin Zhou, Wei An, Weidong Sheng, and Li Liu. Visible-thermal tiny object detection: A benchmark dataset and baselines. *arXiv preprint*, 6 2024.

[91] Zhiqiang Zeng, Jinping Sun, Zhu Han, and Wen Hong. SAR automatic target recognition method based on multi-stream complex-valued networks. *IEEE Trans. Geosci. Remote Sens.*, 60:1–18, 2022.

[92] Yikui Zhai, Wenlve Zhou, Bing Sun, Jingwen Li, Qirui Ke, Zilu Ying, Junying Gan, Chaoyun Mai, Ruggero Donida Labati, Vincenzo Piuri, and Fabio Scotti. Weakly contrastive learning via batch instance discrimination and feature clustering for small sample SAR ATR. *IEEE Trans. Geosci. Remote Sens.*, 60:1–17, 2022.

[93] Honglei Zhang, Wenpeng Zhang, Yongxiang Liu, Wei Yang,

and Shaowei Yong. Scatterer-level time-frequency-frequency rate representation for micro-motion identification. *Remote Sens.*, 15(20):4917, 2023.

[94] Jinsong Zhang, Mengdao Xing, and Yiyuan Xie. FEC: A feature fusion framework for SAR target recognition based on electromagnetic scattering features and deep CNN features. *IEEE Trans. Geosci. Remote Sens.*, 59(3):2174–2187, 2020.

[95] Linbin Zhang, Xiangguang Leng, Sijia Feng, Xiaojie Ma, Kefeng Ji, Gangyao Kuang, and Li Liu. Optimal azimuth angle selection for limited SAR vehicle target recognition. *ISPRS J. Photogramm. Remote Sens.*, 128:103707, 2024.

[96] Xiaosong Zhang, Yunjie Tian, Lingxi Xie, Wei Huang, Qi Dai, Qixiang Ye, and Qi Tian. HiViT: A simpler and more efficient design of hierarchical vision transformer. In *Proc. Int. Conf. Learn. Represent. (ICLR)*, 2023.

[97] Xinzheng Zhang, Yuqing Luo, and Liping Hu. Semi-supervised SAR ATR via epoch- and uncertainty-aware pseudo-label exploitation. *IEEE Trans. Geosci. Remote Sens.*, 61:1–15, 2023.

[98] Jie Zhou, Chao Xiao, Bo Peng, Zhen Liu, Li Liu, Yongxiang Liu, and Xiang Li. DiffDet4SAR: Diffusion-based aircraft target detection network for SAR images. *IEEE Geosci. Remote Sens. Lett.*, 2024.

[99] Kaiyang Zhou, Ziwei Liu, Yu Qiao, Tao Xiang, and Chen Change Loy. Domain generalization: A survey. *IEEE Trans. Pattern Anal. Mach. Intell.*, 45(4):4396–4415, 2023.

[100] Xingyi Zhou, Dequan Wang, and Philipp Krähenbühl. Objects as points. *arXiv preprint*, 2019.

[101] daiyin Zhu, zhe geng, xiang yu, shengliang han, weixing yang, jiming lyu, zheng Ye, and He yang. SAR database construction for ground targets at multiple angles and target recognition method (in chinese). *J. Nanjing Univ. of Aeronaut. Astronaut.*, 54(5):985–994, 2022.